OBSERVATIONS OF DIURNAL MELT-FREEZE EVENTS USING TIME DOMAIN REFLECTOMETRY (TDR) IN SEASONAL SNOWPACK

by

Brittany Gold

A thesis submitted to the faculty of
The University of Utah
in partial fulfillment of the requirements for the degree of

Master of Science

Department of Geography

The University of Utah

August 2014

The University of Utah Graduate School

STATEMENT OF THESIS APPROVAL

The thesis of **Brittany Gold**

has been approved by the following supervisory committee members:

Richard Forster	, Chair	**April 30, 2014** Date Approved
Phoebe McNeally	, Member	**April 30, 2014** Date Approved
John Petersen	, Member	**May 9, 2014** Date Approved

and by **Andrea Brunelle**, Chair/Dean of

the Department/College/School of **Geography**

and by David B. Kieda, Dean of The Graduate School.

ABSTRACT

Understanding seasonal snowpack characteristics is essential for avalanche forecasting and water resource management. As technology advances, instruments continue to be developed to study seasonal snowpack characteristics. These instruments range from ultrasonic snow depth sensors to microwave sensors flown on satellites to sensors based on snow's electrical properties. Few studies have looked at time domain reflectometry's (TDR) applicability to measure dry snow density and daily fluctuations in liquid water content due to diurnal melt-freeze cycles. This study aims to build on previous TDR studies of seasonal snowpack and assess the effectiveness of a TDR system to monitor diurnal changes in snowpack liquid water content.

Results are from a test springtime snowpit in Alta, UT. Measured snow densities range from 108kg/m^3 to 414kg/m^3 with a measurement error of 4%. Through the comparison of manually measured densities and dielectric values from the TDR, insight into the TDR's applicability to density measurements is gained. Daily fluctuations in the TDR probe dielectric measurements indicate the TDR's applicability to study diurnal melt-freeze cycles. Correlation of diurnal dielectric constant measurements with solar radiation and air temperature suggest that the TDR is able to monitor effects of energy fluxes in the snowpack associated with energy received due to daytime temperatures and shortwave radiation. Calculated liquid water content varied from 1.0 to 2.5 vol. % during diurnal fluctuations, consistent with ranges from previous studies indicating TDR's

applicability to monitor liquid water content in a wet snowpack during melt-freeze transitions.

TABLE OF CONTENTS

LIST OF TABLES

Table

ACKNOWLEDGEMENTS

I would like to thank my advisor Dr. Richard Forster for his support and guidance throughout the thesis process. I am grateful for Dr. Forster's patience and advice, especially during the data analysis portion of my thesis. I would also like to thank my committee members Dr. Phoebe McNeally and Dr. John Petersen. Dr. McNeally was integral in obtaining a relationship with Utah Department of Transportation (UDOT) that allowed me to use a section of their study plot to obtain data. In addition, Dr. McNeally's relationship with UDOT allowed me to easily obtain additional data from UDOT operated sensors. Dr. John Petersen offered guidance through any issues that I encountered with configuring the TDR and datalogger. Dr. Petersen fostered a relationship with Campbell Scientific Inc. that allowed me the opportunity to quickly begin a new project with a different sensor when we hit a roadblock with the initial project. I am very grateful to Campbell Scientific Inc. for the opportunity to borrow equipment essential to the data collection portion of my research. I would also like to thank UDOT for the protected study plot space, auxiliary data, and the use of equipment. Lastly, I would like to thank the Donald R. Currey Scholarship for funds used to obtain equipment essential to my research.

CHAPTER 1

INTRODUCTION AND LITERATURE REVIEW

1.1 Introduction

Understanding snowpack conditions is vital for snowmelt runoff modeling as well as avalanche assessment. Manually monitoring snowpack conditions is becoming increasingly expensive, which lends increased importance to developing accurate and encompassing automated techniques (Lundberg, Granlund, & Gustafsson, 2010). Over the past few decades, technology in conjunction with improved techniques has helped enhance understanding of seasonal snowpack characteristics.

Snowpack observations that were once taken by hand are now measured with automated devices, such as ultrasonic depth sensors and snow pillows. Technological advancements have allowed increased accuracy in measuring snowpack characteristics, such as snow water equivalent (SWE) and stratigraphy, which plays an important role in the timing of snowmelt. Snowpack characteristics across the globe are now monitored from a distance and used as inputs for runoff models. These runoff models assist water resource management with the predictions of springtime flooding, domestic and agricultural water supply in regions that rely on snowmelt for water, and hydropower planning (Lundberg et al., 2010).

Understanding the spatial and temporal nature of snowpack characteristics and layers has many applications, especially for wet avalanche forecasting. Knowledge of

liquid water onset and propagation through the snowpack may assist with forecasting wet avalanches (Baggi & Schweizer, 2009; Katsushima, Yamaguchi, Kumakura, & Sato, 2013; Kattelmann, 1985). Point observations of liquid water content and other snowpack characteristics are used to calibrate instruments, such as microwave radars and Light Detection And Ranging (LIDAR), that may measure snow water equivalent (SWE) or snow covered area (Waldner, Huebner, Schneebeli, Brandelik, & Rau, 2001). The use of ground- and satellite-based snow cover observations as well as techniques, such as Time Domain Reflectometry (TDR), may help predict where and when avalanches will occur, potentially saving lives and money.

Snowfall is the source for 75% of the western United States' annual water supply (Doesken & Judson, 1997; Ryan, Doesken, & Fassnacht, 2008). Understanding mechanisms, such as diurnal melt-freeze cycles and the downward propagation of liquid water through the snowpack, that affect snowmelt timing is important for water supply management. The following study will use the TDR method (described in detail in Chapter 2) to understand how solar radiation, air temperature, snow density, and snow liquid water content interact during diurnal melt-freeze cycles in a snowpack. This thesis will discuss previous research and principles behind Time Domain Reflectometry (TDR) used in snowpack studies. Objectives and the methodology utilized to study diurnal melt-freeze events, correlation between measured dielectric constant and solar radiation and air temperature, and liquid water content in the snowpack are addressed. It will conclude with results from this study, a discussion of these results in the context of prior research and conclusions.

1.2 Literature review and background on snowpack's electrical properties

Liquid water content has been successfully measured with several laboratory-based methods, such as freezing calorimtery, centrifugal separation, and the dilution method (i.e., Lundberg et al., 2010; Techel & Pielmeier, 2011). Field-based measurements of liquid water content and dielectric constant have been performed with snow fork, Denoth meter, and TDR. These field-based methods will be discussed in this chapter; special attention will be paid to the operation of and studies that use TDR.

1.2.1 Capacitance sensors

The snow fork and Denoth meter are capacitive sensors, which can determine the snowpack's density and wetness once inserted into the snowpack (Lundberg et al., 2010; Sihvola and Tiuri, 1986). Neither the snow fork nor the Denoth meter are suitable for automated temporal monitoring of snowpack wetness and density. The snow fork requires an observer to manually insert the fork into the snowpack for each measurement. The Denoth meter consists of a plate that when inserted into the snowpack absorbs additional solar radiation causing increased melting or warming. In addition, the Denoth meter blocks the percolation of water through the snowpack and may record increased liquid water content due to pooling if left in the snowpack for extended campaigns (Techel & Pielmeier, 2011). If temporal monitoring of snowpack wetness and density are desired then the TDR method either with a Snowpower Band or probes will be less disruptive to the natural snowpack processes than capacitive sensor methods.

1.2.2 Key concepts in measuring snowpack's electrical properties

An understanding of several key electrical terms needs to be achieved in order to understand how the TDR can be applied to study snowpack characteristics. This section will review terms, such as dielectric constant, and the components of snow that lend it to being an effective insulator. These terms and concepts will form the basis for understanding how the TDR method can be successfully applied to snowpack studies.

The snowpack can be referred to as an electrical insulator since an electric field can polarize this dielectric material. A dielectric material is typically highly polarizable. Clean wet snow is comprised of ice, water, and air. Water, the liquid state of ice, is a polar molecule (Figure 1.1), which has a partial positive charge on one side and a partial negative charge on the other side (Dielectric Constant, 2012). These partial positive and negative charges are known as dipoles, which in the case of water, result in a net dipole.

The polarizability of a material can be measured by the material's dielectric constant. The dielectric constant consists of a real and an imaginary part. The imaginary part of the dielectric constant of snow is related to wetness, while the real part of the dielectric constant of snow is a function of both density and wetness *(*Dielectric Constant*,* 2012; Rikkers, personal communication, January 14, 2013). According to Rikkers, the dielectric constant of snow is the weighted average of the dielectric constant of its three components. The TDR method is able to measure the dielectric constant of snow.

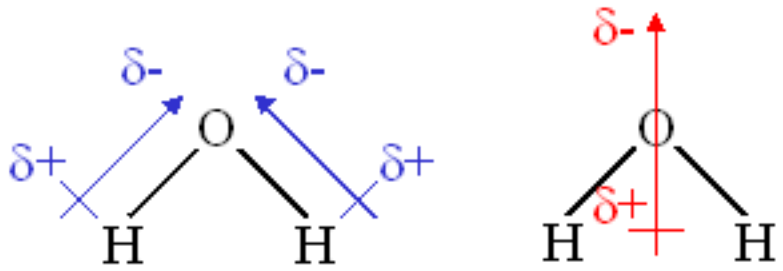

Figure 1.1: This diagram shows the net dipole for a water molecule.

1.2.3 Recent TDR and related dielectric studies

Since Stein and Kane's first study (1983), there have been few other studies that experiment with the TDR method's applicability to snowpack studies. This section reviews several TDR and related snowpack studies from the 1980s to present day.

In 1983, Stein and Kane performed the first field experiment using a TDR and probes (Figure 1.2) to continuously monitor liquid water content in soil. This study also experiments with the use of TDR to monitor snowmelt infiltration into frozen soils as well as liquid water propagation through the snowpack. Stein and Kane initially believed that the liquid water content of snow could be found by measuring the dielectric constant of snow and by using Topp's relationship (Appendix A). Through their experiments, they conclude that even when liquid water is not present in the snowpack, the dielectric constant varies considerably due to snow density. They also note an increase in the dielectric constant due to an increase in the liquid water content and an increase in snow density. They notice difficulty in determining the value of liquid water content in snow due to the measured dielectric constant's dependency on both snow density and liquid water content (Stein & Kane, 1983).

Following Stein and Kane's 1983 study, the next advancement in TDR

Figure 1.2: The TDR (top) can be attached to probes (bottom) and inserted into the snowpack (or soil) in order to take measurements of snow density and wetness. Adapted from campbellsci.com.

applications to snowpack studies is Stein, Laberge, and Lévesque (1997) on the relations between snow liquid water content, snow density, and dielectric constant. This study compares the dielectric constant, liquid water content and snow density from the freezing calorimetry (Appendix B) and TDR techniques (Stein et al., 1997). This study tests several different probe designs that could be used to continuously measure snow liquid water content. They conclude that with a dry snowpack, the dielectric constant of the measured snow is dependent only on the snow density (Stein et al., 1997). They suggest using probes containing rods with a diameter smaller than 0.6 cm to eliminate the issue of rods influencing the densification process of the snowpack (Stein et al., 1997).

Lundberg (1997) also compares laboratory dilution methods (Appendix C) to laboratory TDR measurements to assess the accuracy of the TDR technique to measure liquid water content. Lundberg concludes that the TDR technique has the ability to measure variations in snow liquid water content down to 1–2 volume %. Lundberg also concludes that snowpack liquid water content could be continuously measured in the field with a spatial resolution of 5 cm with the use of several sets of probes.

Following these 1997 studies, Waldner et al. (2001) use a capacitance sensor (Figure 1.3) to determine the spatial variability of water content in the snowpack. They extract snow from a 16 m wide and about 0.5 m deep snowpit. Measurements taken with this capacitance sensor are recorded for 2 consecutive days at a depth of about 0.5 m below the snow surface and with 1-m spacing. Waldner et al. (2001) found fluctuations in liquid water content from 2.5 vol. % to 8.5 vol. % in July that can be attributed to daily melt cycles, and they note fluctuations and lag of liquid water content with solar radiation and air temperature, but do not quantify these correlations or lags.

The Snowpower Band, a modified TDR system, was recently developed in 2004 for the simultaneous measurement of snow density, snow water equivalent (SWE) and liquid water content (Lundberg et al., 2010; Stähli et al., 2004). The dielectric constant of snow can be measured at multiple frequencies by the Snowpower Band (Lundberg et al., 2010; Niang et al., 2006; Stähli et al., 2004). The Snowpower Band was tested at a high-alpine Swiss Site (Stähli et al., 2004) and in an agricultural field in Canada (Lundberg et al., 2010; Niang et al., 2006). The tests in Switzerland were robust, but air pockets formed around the cable due to wind-induced vibrations (Lundberg et al., 2010; Stähli et al., 2004). The sensor cable is large and may disturb the snowpack through contact and absorption of solar radiation (Lundberg et al., 2010).

The most recent study involving the use of a TDR to measure snowpack characteristics is Stacheder's 2005 study. This study uses Snowpower Bands, which are 6-cm wide polyethylene bands containing three copper wires mounted both horizontally and diagonally through the snowpack, to monitor density, liquid water content, and SWE in the snowpack (Figures 1.4 and 1.5). Stacheder finds fairly accurate density

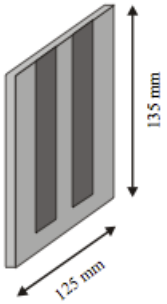

Capacitance sensor
(Denoth, 1994)

Figure 1.3: Example of sensor used in Waldner et al.'s 2001 study of spatial variability in snowpack's liquid water content. Adapted from Waldner et al. (2001).

measurements from the TDR compared to manual measurements with a snow cutter and scale. Stacheder's study also results in plausible liquid water content measurements. During the study, there is not any liquid water present in the snowpack until the snowpack reaches its maximum depth and temperatures begin to rise in early April (Stacheder, 2005). Once liquid water is present in the snowpack, Stacheder notes steadily increasing liquid water content due to increases in the dielectric constant, indicating the downward penetration of the melting front. He also notices trends in the liquid water content according to diurnal melt-freeze cycles (Stacheder, 2005). Lastly, depth and density measurements result in encouraging SWE results (Stacheder, 2005).

The most recent study based on snowpack's electrical properties is Techel and Pielmeier's study (2011). Thousands of spatial measurements of snow liquid water content using snow fork, Denoth meter, and the hand squeeze test were performed in their snowpack wetness study. They measured and compared spatial and temporal changes in liquid water content with these methods. They noted large diurnal changes in wetness, especially within the uppermost 10 cm of the snowpack (Techel & Pielmeier, 2011).

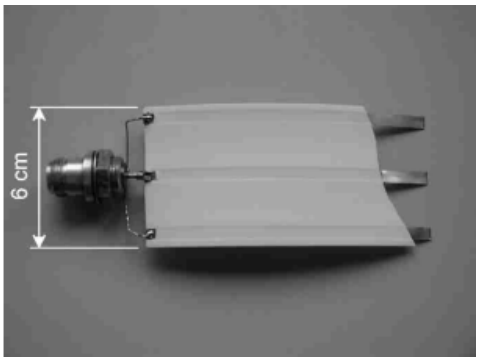

Figure 1.4: The image is a small section of the polyethylene band that Stacheder used in his 2005 study. The three copper wires are visible. Adapted from Stacheder (2005).

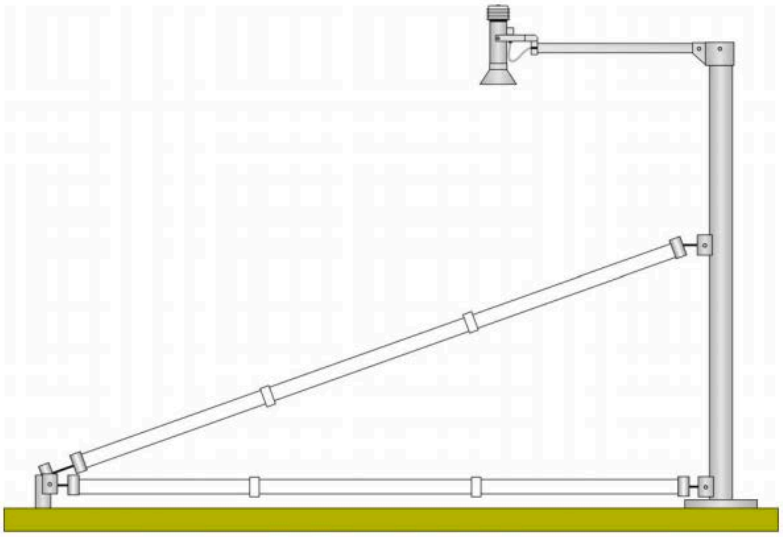

Figure 1.5: This figure shows the Snowpower Bands mounted horizontally and diagonally, similar to the field setup Stacheder (2005). Adapted from http://sommer.at

They conclude that these methods work well at tracking changes in snowpack wetness, but their measurements "…do not allow a conclusive interpretation on the accuracy of the measured water content" (Techel & Pielmeier, 2011).

1.2.4 Snowpack energy balance budget

Understanding the energy balance budget of the snowpack is essential to identifying melt processes within the snowpack. The total energy balance of the snowpack is determined by the total energy flux equation (1.1):

$$\partial U_i/\partial_t = Q_s + Q_l + Q_h + Q_e + Q_a + Q_g - Q_m \quad (1.1)$$

from shortwave radiation (Q_s), longwave radiation (Q_l), convection of sensible heat (Q_h), convective transfer of latent heat due to condensation (Q_c), sensible heat from rain (Q_a), and conduction of heat from soil (Q_g; Figure 1.6).

Although these six heat exchanges all contribute to the total energy balance budget of the snowpack, shortwave radiation in the form of solar radiation accounts for about 60% of the energy received by the snowpack (R. Julander, personal communication, January 8, 2014). Longwave radiation, typically reflected radiation from the sky, clouds, and/or vegetation accounts for about 10% of the energy needed for snowmelt. The remaining 30% of energy needed for snowmelt comes from the remaining heat exchange processes including heat exchange between the snowpack and the overlying air mass. Convection of sensible heat is essentially the heat exchange between the snowpack and the overlying air mass, which is controlled by the air temperature gradient and wind speed. Convective transfer of latent heat due to condensation, which occurs where warm moist air masses are present or there is condensation during a rain on snow event, and is dictated by vapor pressure gradient and wind speed. Sensible heat from rain, which is

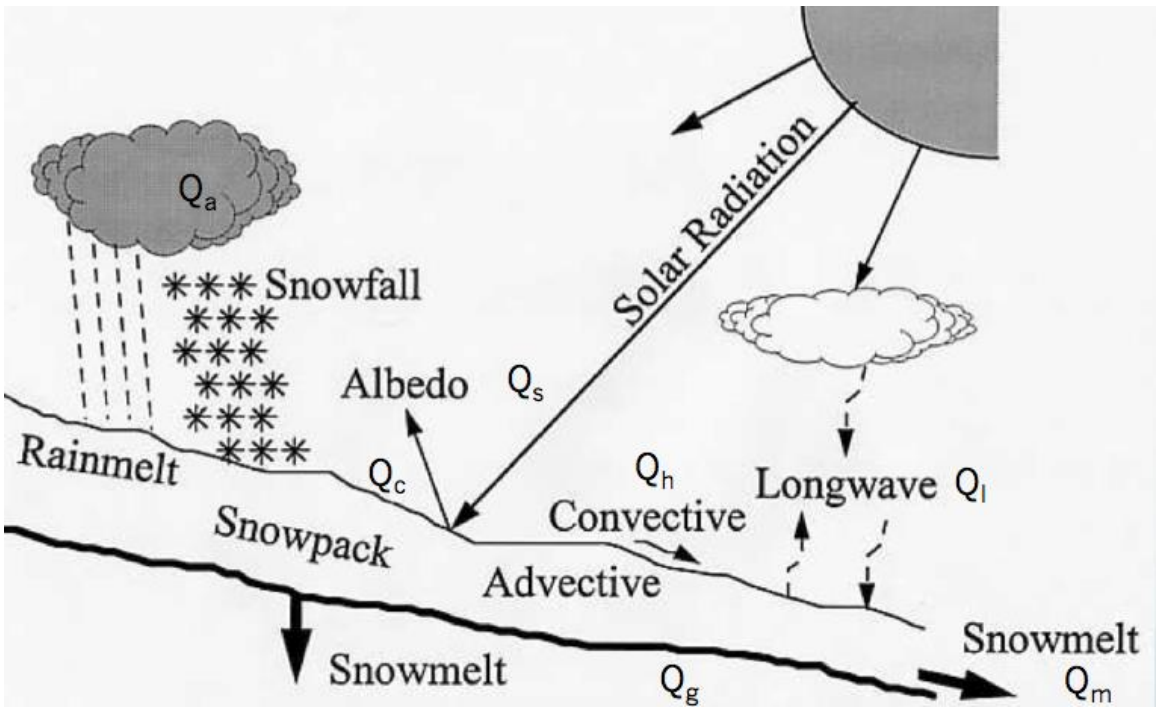

Figure 1.6: This is a diagram of the energy exchange between the snowpack and its surroundings. Adapted from Assaf (2007).

typically very low, especially in Utah, introduces additional heat into the snowpack. Lastly, conduction of heat from soil introduces additional small quantities of energy into the snowpack.

Although there are several heat exchange processes that impact the snowpack's energy balance budget, and ultimately the onset of snowmelt, solar radiation is the largest contributor. Solar radiation data are collected at various snow and weather observation sites around the United States. Air temperature is not a significant energy input into the snowpack, but it still has an influence on the snowpack's overall energy balance budget. Air temperature data are available for virtually any populated place around the United States as well as weather and snow observation sites across the country. Both solar radiation and air temperature data are readily available.

CHAPTER 2

OBJECTIVES AND METHODOLOGY

This chapter will discuss the objectives and methodology used in this study. The overarching objective of this study is to test various implementations of the TDR for snowpack characterization. There are key differences between previous TDR snowpack characteristic studies and this study. Lundberg's (1997) study was based in a laboratory; this study will take field measurements in order to assess real-world conditions of an evolving snowpack. Stein et al. (1997) used probes with different diameters, lengths, and electrical properties, while this study will use probes with the same configuration for all experiments, which may lend itself to more widespread use. Waldner et al. (2001) noted an association and an offset amongst snow liquid water content, solar radiation, and air temperature; this study observes the correlation between the measured snowpack dielectric constant and energy balance budget inputs. Stacheder (2005) measured the bulk dielectric constant for the entire snowpack, while this study measures the dielectric constant within different layers in the snowpack. Techel and Pielmeier (2011) used the snow fork, Denoth meter, and hand squeeze test to detect the spatial and temporal evolution of liquid water content. This study will use a TDR to observe the temporal evolution of the dielectric constant and liquid water content in the snowpack.

2.1 Objectives

The TDR and probe design, discussed in section 2.2.1, will be used to meet the following objectives:

1) Measure real-time density in a dry snowpack
2) Track the downward propagation of liquid water through the snowpack
3) Monitor diurnal melt-freeze cycles according to increases and decreases in dielectric constant
4) Correlate observed diurnal cycles in the measured dielectric constant with solar radiation and air temperature data
5) Obtain liquid water content estimates in an isothermal snowpack.

It is hypothesized that solar radiation is more strongly correlated to dielectric constant than air temperature, and solar radiation will have a greater lag behind dielectric constant than air temperature. Overall, this study assesses how well a TDR and multiple probes are able to assess the temporal evolution of the snowpack with special attention to diurnal melt-freeze cycles and liquid water content.

2.2 Methodology for data collection

This section will include the TDR and probe specifications and data collection timeline, including data collected, site locations, and date descriptions as well as techniques used for data analysis. The snowpack was wet and isothermal during most of the measurement dates. May 19–22, 2013, is the only measured period where daytime temperatures exceed freezing and nighttime temperatures are below freezing. During this period, the snowpack is isothermal and has begun to melt. The density data from May 1

are used to calculate liquid water content for the May 19–22, 2013, period. Dry snow densities recorded on March 22 and November 8, 2013, are used to calculate an offset between measured snow densities and those computed from simultaneous dielectric measurements. This offset is used as a calibration factor when later computing snow wetness values. Table 2.1 shows the dates dielectric constant and density data were collected. Collection of density data and the offset calculation will be discussed in detail in the following section.

Snowpack dielectric constant was measured at the Alta Guard-House Utah Department of Transportation (UDOT) Avalanche snow study plot (Figure 2.1). Air temperature data were downloaded from the same location courtesy of Adam Naisbett of the UDOT Avalanche center. Solar radiation data were obtained from the Parley's Summit UDOT site (Figure 2.1), which is the nearest and most similar site with solar radiation data for the study period of May 19–22, 2013.

2.2.1 General TDR methods for collection of dielectric constant and snow density

This study used the Campbell Scientific TDR100, CS605 probes, and CR1000 datalogger to measure snowpack characteristics. The TDR takes raw measurements by first emitting a high frequency pulse then sampling the waveform of any reflections. The waveform is analyzed, and the travel time of the pulse is determined and then stored in a datalogger or on a laptop (Figure 2.2). The following set of equations is the basis for the density calculation from measured dielectric constant values:

$$D = V * T \tag{2.1}$$

where D is the distance (length) of the probe, V is the velocity of the pulse propagation

Table 2.1: This table shows the time periods data were collected. The wetness of the snowpack is denoted through "dry" and "wet." Time periods are considered dry when liquid water is absent from the snowpack, while time periods are considered wet when liquid water is present in the snowpack. Time periods in which snow density data were collected are also noted. The dielectric constant was recorded either in situ with the laptop or temporally with the datalogger.

Time Period (2013**)**	**Snow Conditions**	**Density Collected?**	**Collection Method**
March 22	Dry	Yes	Laptop
March 28	Wet	Yes	Laptop
April 13	Wet	Yes	Laptop
April 19	Wet	Yes	Datalogger
April 21–24	Wet	Yes	Datalogger
April 25–May 1	Wet	Yes	Datalogger
May 17–25	**Wet**	**No**	**Datalogger**
October 31–November 8	Dry	Yes	Datalogger

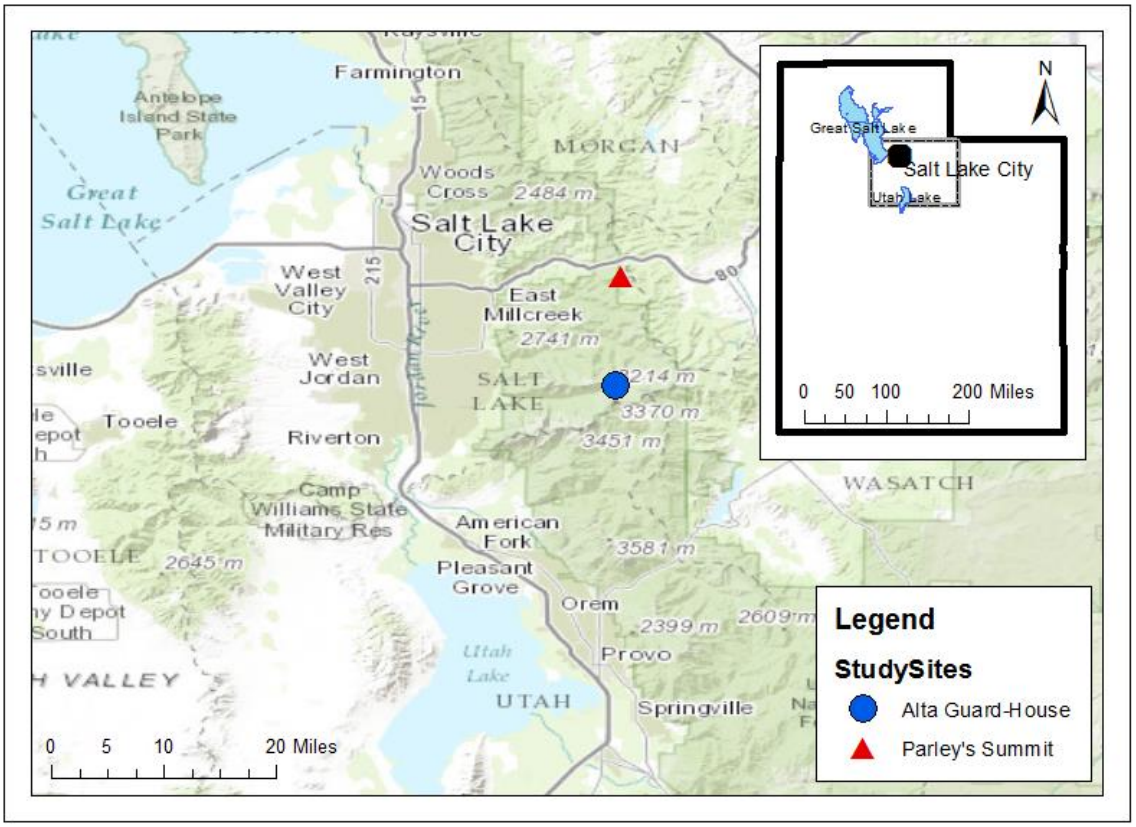

Figure 2.1: This figure shows the locations of the Parley's Summit and Alta Guard-House sites relative to each other as well as in reference to the state of Utah.

through the snow, and T is the propagation time of the pulse from emission to capture.

Distance, or the length of the probe, is known before measurements are taken. The TDR records travel time of the pulse, so the equation can be rewritten to solve for the velocity of the pulse in snow as

$$V = D/T \tag{2.2}$$

The velocity of the pulse through the snow, V, is dependent on the dielectric constant, ε, of the snow around the probe and the speed of light in a vacuum, c.

$$V = \frac{c}{\sqrt{\varepsilon}} \tag{2.3}$$

For dry snow conditions, the dielectric constant, ε, is dependent on the density, ρ, of the

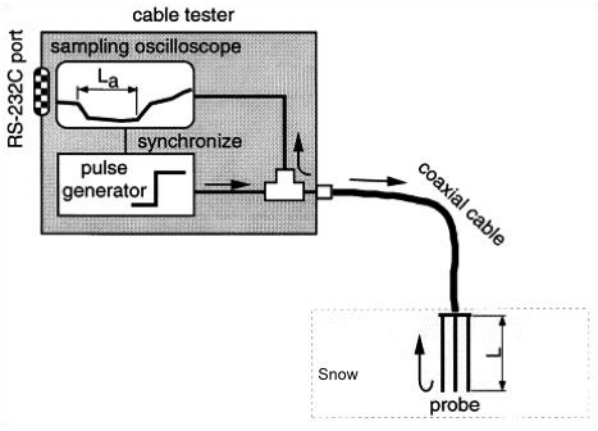

Figure 2.2: This figure is an example of a TDR (left) attached to a probe. L is the length of the probe. Adapted from Noborio (2001).

snow through empirical relationships that have been established by field measurements (Figure 2.3). Tiuri (1984) derived the following equation:

$$\varepsilon = 1 + 1.7\rho + 0.7\rho^2 \tag{2.4}$$

Other equations have been derived from the relationship between dry snow density and measured dielectric constant. Select equations will be discussed in detail in section 2.3.1. By combining equations (2.2), (2.3), and (2.4), dry snow density can be calculated from the travel time measured by the TDR.

For a wet snowpack, one containing liquid water, the dielectric constant is affected by a combination of snow density and liquid water content. Therefore, in order to detect liquid water in the snowpack, changes in the dielectric constant are monitored. The presence of liquid water in the snowpack causes large changes in the dielectric constant. The vertical propagation of liquid water through the snowpack can be tracked with the TDR configuration in Figure 2.4. The pink dye in Figure 2.5 shows the downward propagation of water through the snowpack as well as the formation of Table 2.2. Dry snow is a combination of air and ice, which have a relatively low dielectric

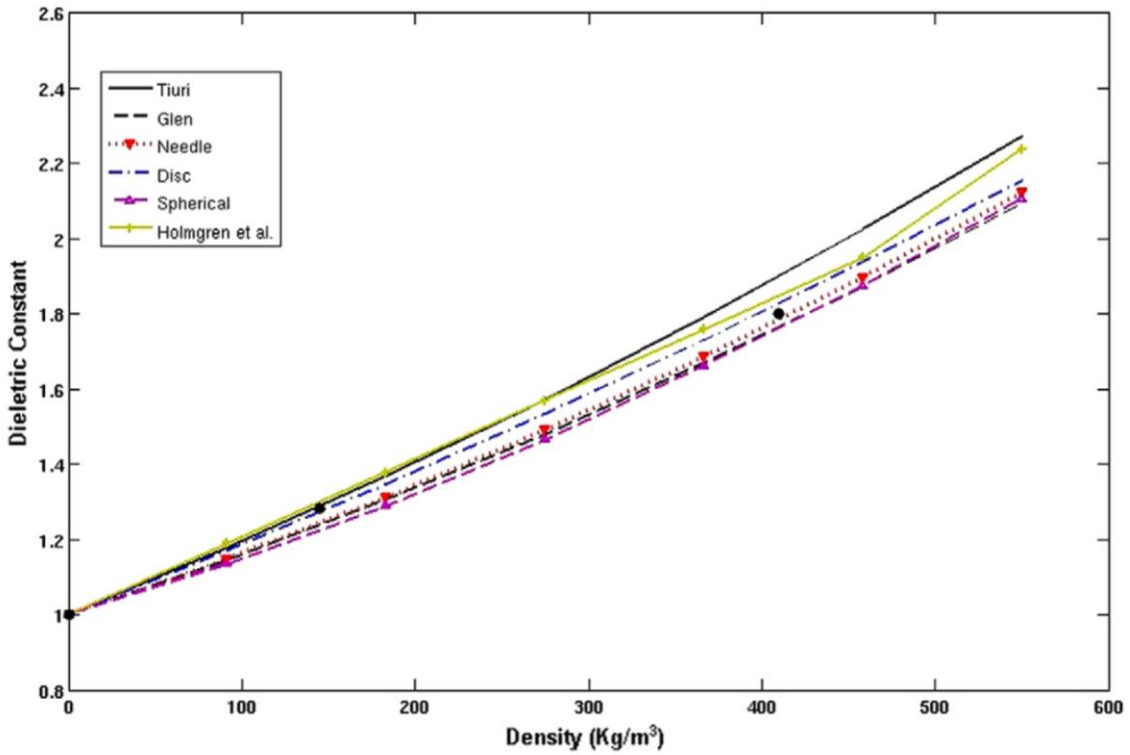

Figure 2.3: This graph shows empirical and theoretical relationships between snow density and dielectric constant. Adapted from Lee and Wang (2009).

constant compared to that of water. Therefore, when liquid water is present in the snowpack, the dielectric constant is greater than when liquid water is not present in the snowpack.

The following subsections will discuss the methodology that will be used to meet the objectives outlined in section 2.1.

2.2.2 Data collection of dielectric constant and snow density

In order to measure the dielectric constant in the snowpack with the TDR, north-facing snow pits were excavated to a depth of 100 cm. Eight probes were inserted horizontally into the snowpack, starting at the snow surface and proceeding toward the

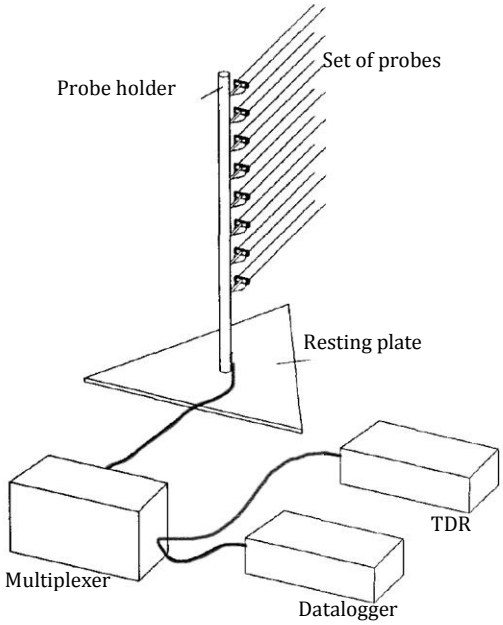

Figure 2.4: This diagram illustrates an experimental configuration with evenly spaced probes that can be inserted into the snowpack to track the downward propagation of liquid water through the snowpack. Adapted from Lundberg (1997).

Figure 2.5: The pink dye in the image shows the downward propagation of liquid water through the snowpack as well as preferential flow paths. Changes in the dielectric constant will indicate increases or decreases in the presence on liquid water in the snowpack. Adapted from Campbell et al. (2005).

Table 2.2: This table compares the dielectric constant of snow's constituents—air, ice, and water.

Material	**Air**	**Ice**	**Water**
Dielectric Constant (ε)	1	3.2	88

ground with 10-cm spacing (Figure 2.6). The TDR responses were recorded with either a datalogger (Figure 2.7) or a laptop computer. In order to assess uncertainty with TDR measurements, multiple TDR measurements in the air were recorded, and the standard deviations of the TDR's multiple dielectric constant measurements were calculated.

In order to assess the accuracy of the TDR snow density measurements, manual density measurements were taken directly after TDR probe density measurements were recorded. Within each homogeneous density layer, two to three manual density measurements were taken with a snow cutter and scale (Figure 2.8). Error for density measurements was measured the same as before using the standard deviation from two to three measurements. Figure 2.9 shows what the snowpit may look like once manual density measurements have been taken. The TDR responses and manual measurements were then compared using methods from Coléou (1998), described in detail in section 2.3.1.

The last part of the data collection methodology for this project was to qualitatively track the propagation of liquid water through the snowpack. As with the previous methodology, a snow pit was excavated to a depth of 100 cm, and eight probes were inserted horizontally into the snowpack evenly spaced throughout the depth of the snowpit (Figures 2.4 and 2.10). The pit was backfilled, burying the probes beneath the snow, and the datalogger was used to record the TDR responses.

Figure 2.6: An example of inserting the probe horizontally into the snowpack.

Figure 2.7: The above image is the datalogger used to record dielectric constant data. Adapted from campbellsci.com.

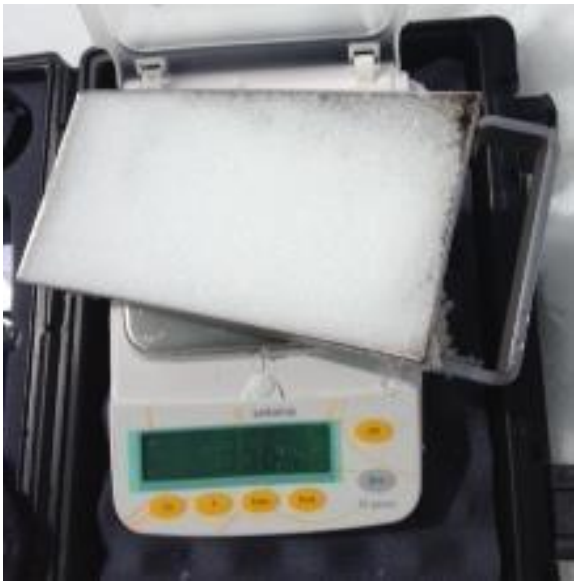

Figure 2.8: The image above shows the snow cutter on top of the scale. The known volume of snow in the snow cutter will be used to manually measure snow density.

Figure 2.9: This is an image of a snowpit once manual density measurements have been taken throughout the depth of the snowpit.

Figure 2.10: The setup for tracking the temporal evolution of snow density. The probes are horizontally placed into the snowpack 10 cm apart.

2.3 Data analysis

This section will review the techniques used in this study to analyze dry snow dielectric constant and offset calculations; evaluate diurnal melt-freeze events with measured dielectric constant; correlate diurnal melt-freeze cycles amongst the dielectric constant, solar radiation, and air temperature; and calculate snow liquid water content. Mätzler (2.5), Looyenga (2.6), and Tiuri's (2.4; discussed in 2.2.1) equations, which have established a relationship between the dielectric constant and dry snow density, were used to calculate an offset for the dielectric constant measured by the probe when liquid water is present in the snowpack will be reviewed. Lastly, Denoth's (1994) equation, which establishes a relationship between snow dielectric constant, density, and liquid water content, will be reviewed.

2.3.1 Dry snow density and dielectric constant offset calculation

Mätzler (1996) established a formula, (2.5), that converts measured dry snow density to a dielectric constant.

$$\varepsilon'_{ds} = 1 + \frac{1.58\rho_{ds}}{1 - 0.365\rho_{ds}} \tag{2.5}$$

where ε'_{ds}, the dielectric constant of snow, and ρ_{ds}, the density of dry snow, have been found to be more accurate on snow densities less than 400kg/m^3 (Mätzler, 1996). Looyenga's (1965) formula (2.6)

$$\varepsilon_d = (\theta_i\, \varepsilon_i^{1/3} + \theta_w\, \varepsilon_w^{1/3} + \theta_a \varepsilon_a^{1/3})^3 \tag{2.6}$$

where ε_d is the dielectric constant of snow; θ_i , θ_w , and θ_a are the volumetric contents of ice, water, and air, respectively; and ε_i, ε_w, and ε_a are the known dielectrics of ice, water and air, respectively, is more accurate on densities approaching that of firn and ice, densities greater than 400kg/m^3 (Waldner et al., 2001). Manually measured dry snow densities did not exceed 400kg/m^3, so Looyenga's formula was not used in data calculation, but was considered in conceptualization. Mätzler and Tiuri's formulas (2.4) were used to assess how well observed TDR and probe measurements compare with theoretical dielectric values. The dielectric and density values obtained with Mätzler and Tiuri's formulas for all measured snow densities were assessed. Visual graphical data and analysis of error were used to analyze how well the experimental data fit the theoretical data.

According to methods from Coléou (1998), the average difference between the average of the Mätzler and Tiuri's formulas' dielectric constant calculation based on measured densities and the measured dielectric constant will yield an offset. This offset

can later be applied to wet snow dielectric constant measurements as a calibration factor in order to yield a dielectric constant value that more realistically represents the snow wetness.

2.3.2 Diurnal melt-freeze cycles and correlation and lag with solar radiation and air temperature

In order to assess how well the TDR was able to capture qualitative changes in the dielectric constant due to diurnal melt-freeze cycles, time series plots of dielectric constant adjusted with the offset described above were created. These graphs indicate if the TDR is able to qualitatively monitor increases and decreases in liquid water content due to daily temperature and solar radiation fluctuations. In addition, an increasing dielectric constant within each homogeneous snowpack layer as well as for all snowpack layers indicate if the TDR is able to track liquid water propagation through the snowpack, and/or the onset and duration of melting. Linear regression between the measured dielectric constant at 10-cm and 80-cm depths was assessed at lags between 0 and 3 hours in order to assess if there is a measurable offset between liquid water in the top of the snowpack and liquid water at an 80-cm depth.

In order to assess the correlation and lag between the measured dielectric constant for the 10-cm probe and diurnal melt-freeze cycles, linear and multiple linear regression were performed. Correlation and lag between solar radiation and the dielectric constant and between air temperature and the dielectric constant was assessed using linear regression at lags between 0 and 10 hours for all possible 24- and 48-hour periods from noon to noon and midnight to midnight between May 19, 2013, at midnight and May 22,

2013, at midnight. Correlation and lag between solar radiation and air temperature and the dielectric constant was assessed using multiple linear regression for all lag combinations between 0 and 10 hours for the same time periods. Finally, correlation and lag between solar radiation and air temperature at lags between 0 and 3 hours were assessed using linear regression for the same time periods. The correlation coefficients obtained from this method can be used to assess if the melting and refreezing of the snowpack is associated with increases and decreases in solar radiation and air temperature.

2.3.3 Liquid water content calculations using Denoth's (1994) equation

Denoth (1994) experimentally collected long-term variations in snow wetness during diurnal cycles. These data were used to empirically establish a relationship amongst snow dielectric constant (ε), snow density (ρ g/cm^3), and snow wetness (θ vol. %). The following equation, (2.7), is applied to manual snow density measurements and recorded dielectric constant measurements to obtain liquid water content in certain snowpack layers:

$$\varepsilon = 1 + 1.92\rho + 0.44\rho^2 + 0.187\theta + 0.0045\theta^2 \qquad (2.7)$$

This equation was used to calculate liquid water content from manual density measurements made on May 1, 2013, and dielectric constant data collected between May 19 and May 22, 2013. Time series plots of liquid water content, air temperature, and solar radiation as well as comparison with previous studies indicates if the calculated liquid water content is reasonable.

2.3.4 Data quality

Special attention was paid to manual density and automated probe measurements to assure accurate data gathering. To ensure high-quality density measurements, at least two density measurements with the snow cutter and scale were recorded for each layer in which dielectric measurements from the probe were recorded. These two to three density measurements were averaged and assessed for uncertainty in measurements. The data collector ensured that the snow cutter was completely full of snow without foreign material, such as plant matter, but not overfilled before weighing the snow cutter with the snow scale. In order to estimate the uncertainty in dielectric measurements from the TDR, air measurements for each probe were recorded several times, and standard deviation was calculated.

CHAPTER 3

RESULTS AND DISCUSSION

Manual snow density and dielectric constant measurements were recorded for select periods in March through May, 2013, as well as late October through early November, 2013. These measurements provide insight into the relationship between TDR dielectric measurements and snowpack liquid water content through fluctuations in the dielectric constant due to changes in snow density and liquid water content. Results from TDR method measurements provide increased understanding of energy inputs, such as solar radiation, into the snowpack that affect snowpack diurnal melt-freeze cycles and overall liquid water content. The following sections will discuss results from dielectric constant measurements with regards to density, diurnal melt-freeze cycles, correlation and lag with solar radiation, air temperature, liquid water content, and melt water propagation through the snowpack, as well as the effectiveness of the TDR for snowpack characteristic studies.

3.1 Snow density and dielectric constant offset

Results from previous studies established an empirical relationship between the dielectric constant and dry snow density (Figure 2.3). The majority of the data collected in this study occurred when liquid water was present in the snowpack, violating the relatively simple relationships established between dry snow density and the dielectric

analysis of the dry snow dielectric constant; however, methods from Coléou (1998) suggest that the difference between calculated and observed dielectric constant will yield an offset that can be applied to measured dielectric constant values. Results from this technique will be discussed below as well.

Multiple dielectric constant measurements taken with each probe in the air assessed uncertainty between probes (Table 3.1). The standard deviation of these measurements was found to be 0.01. Figure 3.1 shows the uncertainty in the dielectric constant measured by the TDR for the time period between May 18 and May 22, 2013. Backfilling the pit and the shorter time period of each study period prevented air pockets from forming around the snow. In addition, during compaction and creep, the probes appeared to shift with the moving snowpack, and the compaction sealed any air holes above the probes. Difficulty cleanly extracting the probes from the backfilled pit limited further study of the probe movement within the snowpack. In addition, an Analysis Of Variance (ANOVA) test was conducted between these probe measurements, and it was found that the means of the dielectric constant values measured by each probe are not statistically different and therefore, no bias was due to the probes (Table 3.2).

TDR was used to obtain dielectric constant values that are compared with dielectric constant values computed from measured density values using Mätzler and Tiuri's formulas (Figure 3.2). In dry snow, this study's measured densities ranged from 108kg/m^3 to 414kg/m^3 with an uncertainty of 4% calculated using the relative standard error between density measurements. Measured density values coincide with prior studies' observed density ranges for snow from 100 to 400kg/m^3 (Zhang, 2005). Harper and Bradford performed a study in 2003, finding errors of 10% in their density

Table 3.1: This table includes the dielectric constant values measured for each probe in the air at three separate times.

Probes	1	2	3	4	5	6	7	8	Standard Deviation
Dielectric Constant 1	1.142	1.143	1.147	1.142	1.135	1.144	1.171	1.146	0.011
Dielectric Constant 2	1.145	1.153	1.126	1.162	1.160	1.152	1.150	1.149	0.011
Dielectric Constant 3	1.151	1.150	1.148	1.139	1.143	1.141	1.161	1.158	0.008
									0.010

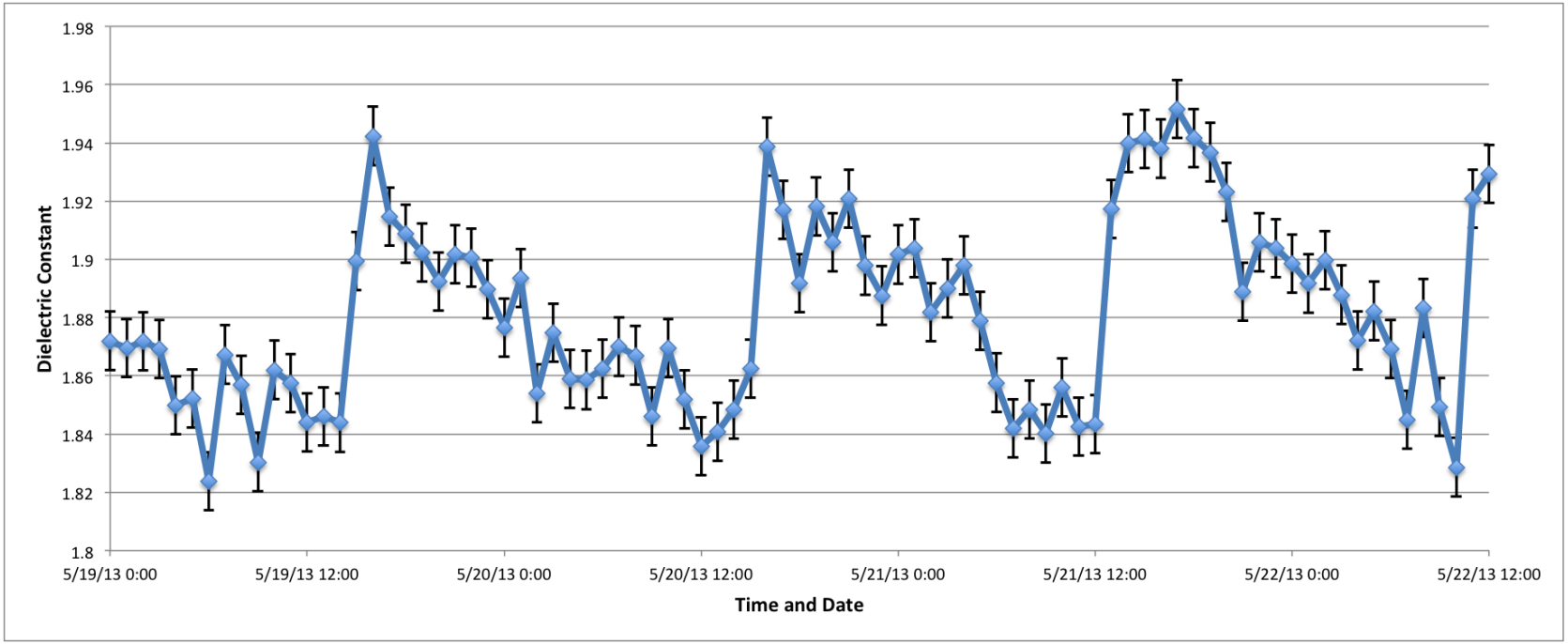

Figure 3.1: The top probe's dielectric constants measured from May 19, 2013, at midnight to May 22, 2013, at noon, and the uncertainty in the dielectric constant measured by the probes are shown here. The uncertainty bar lengths are two standard deviations.

Table 3.2: This table is the results from the ANOVA indicating that the means of the dielectric constant values measured by each probe are not statistically different, and therefore no bias was due to individual probes.

ANOVA						
Source of Variation	*SS*	*df*	*MS*	***F***	*P-value*	***F crit***
Between Groups	0.001	7	0.000	**1.207**	0.354	**2.657**
Within Groups	0.001	16	0.000			
Total	0.002	23				

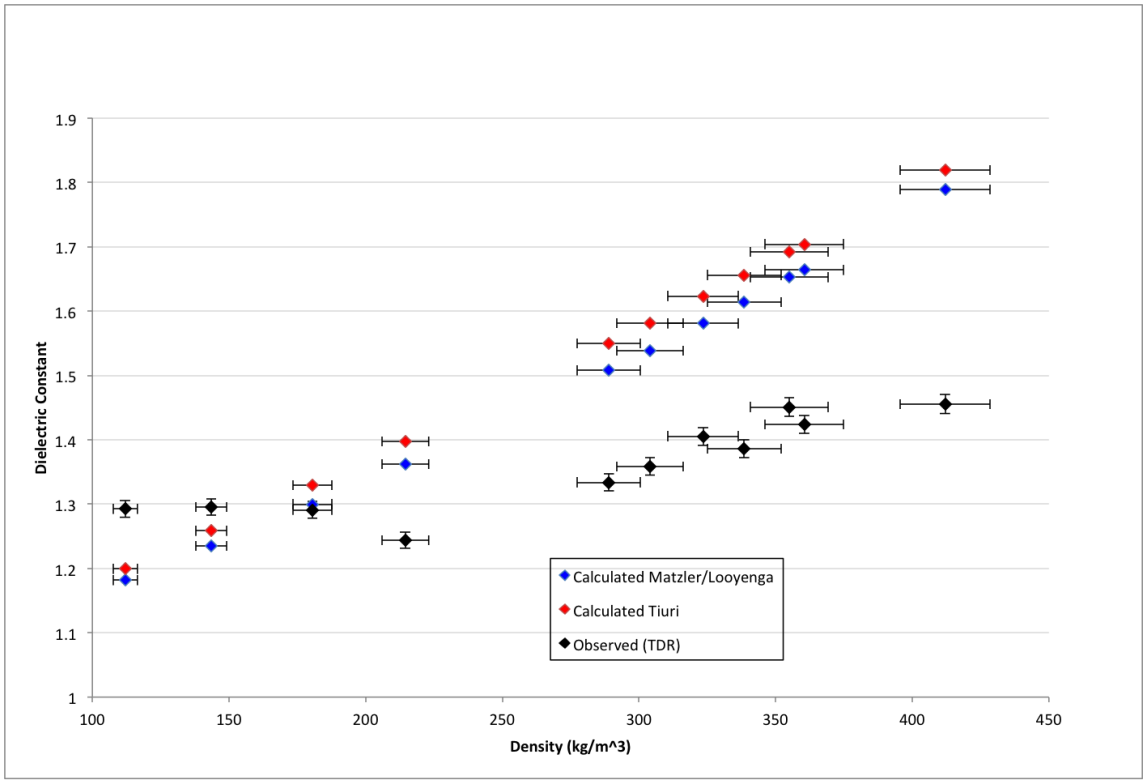

Figure 3.2: This graph shows the comparison of the measured dielectric constant and snow density with the calculated dielectric constant using the average of the measured snow densities. The error bars for the densities are +/- 4%, while the error bars for the observed dielectric are +/- 1%.

measurements. TDR dielectric measurements ranged from 1.29 to 1.48 in dry snow and up to 1.64 in wet snow, which is similar to values recorded in Coléou (1998).

Measured densities were used to compute the dielectric constants (Table 3.3). The relationship between the theoretical dielectric constant and observed density are only valid for dry snow, limiting the amount of data that could be used in this portion of the study to March 22 and November 8, 2013. In addition, the one density measurement greater than 400kg/m^3 yielded unrealistically low dielectric values and was removed from this data (Figure 3.2). Comparison of measured and theoretical dielectric constants reveals an average 11% difference in the dielectric constants measured with the TDR compared to the dielectric constants calculated with Mätzler's equation from the measured density and 12% with Tiuri's formula from the measured density.

Most of this study was conducted in spring, which prevents a direct association between the dielectric constant and density for the majority of data collected. If the snowpack were dry, an increasing dielectric constant, and therefore density due to compaction, would be expected. In a wet snowpack, the increasing dielectric constant demonstrates the increasing presence of liquid water. A direct density measurement cannot easily be obtained from dielectric values in wet snow; however, a qualitative relationship between increased liquid water content and the increased dielectric constant is observed (Figure 3.3). This will be discussed in more detail in section 3.2.

According to methods in Coléou (1998), the average difference between the measured dielectric constant and the dielectric constant values calculated with the average of Mätzler and Tiuri's formulas can be used to obtain an offset that can then be applied to wet snow density. Following this method, an offset of 0.209 was

Table 3.3: This table includes dielectric constant values measured in dry snow as well as the Mätzler and Tiuri calculations of dielectric constant derived from the density measurements. The table also includes the calculation for the overall dielectric constant offset that will later be applied to wet snow dielectric constant measurements.

Dates	Depth below Snow Surface (cm)	Measured Density 1 (kg/m^3)	Measured Density 2 (kg/m^3)	Measured Dielectric 1	Measured Dielectric 2	Measured Dielectric 3	Calculated Mätzler Dielectric 1	Calculated Mätzler Dielectric 2	Calculated Dielectric Tiuri 1	Calculated Dielectric Tiuri 2	Average Measured Dielectric	Average Mätzler and Tiuri	Indiv-idual Offset
22-Mar	10	270	308	1.323	1.347	1.331	1.468	1.547	1.51	1.59	1.334	1.529	0.195
	20	297	311	1.355	1.368	1.353	1.524	1.553	1.567	1.596	1.359	1.56	0.201
	30	323	354	1.394	1.387	1.377	1.579	1.649	1.622	1.69	1.386	1.635	0.249
	40	334	313	1.382	1.435	1.399	1.604	1.558	1.646	1.601	1.405	1.602	0.197
	50	359	362	1.443	1.413	1.415	1.66	1.667	1.701	1.707	1.424	1.684	0.26
	60	328	382	1.46	1.439	1.453	1.59	1.715	1.633	1.752	1.451	1.672	0.222
8-Nov	10	195	234	1.244	1.243	NM	1.326	1.398	1.358	1.436	1.244	1.38	0.136
												Average Offset	**0.209**

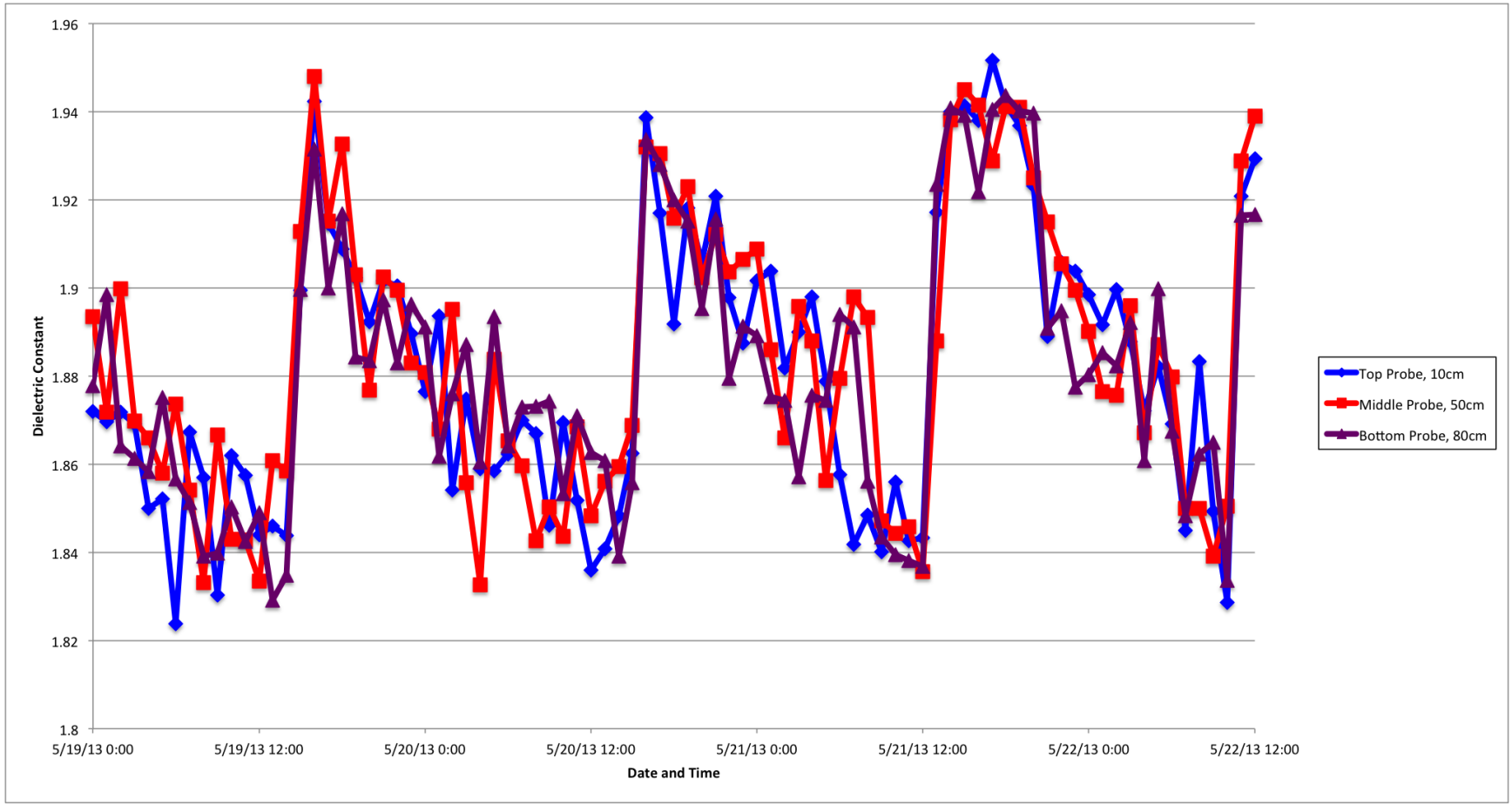

Figure 3.3: Little variation in the dielectric constant values obtained from the top probe at a depth of 10 cm, the middle probe at a depth of 50 cm and the bottom probe at a depth of 80 cm are observed. Additionally, this figure illustrates diurnal cycles in measured dielectric constant.

calculated from the measured dry snow densities and the dry snow dielectric constant (Table 3.3). Coléou's (1998) offset ranging form 0.15 to 0.23 was similar to the offset calculated and applied to the measured dielectric constants in this study.

Due to the relatively small amount of data collected, analysis of dry snow density and dielectric constant data did not support utilizing the dielectric data measured in this study to obtain dry snow density. Several studies require large numbers of dry snow density and dielectric constant measurements to obtain a relationship between dry snow density and the dielectric constant (i.e., Ambach & Denoth, 1972; Cumming, 1952; Frolov & Macheret, 1999; Mätzler 1996). The small sample size limits the use of the TDR to measure dry snow density. The offset obtained using the dry snow density and dielectric constant appears useful since the unadjusted dielectric constant values measured in the wet snow are lower than values that would be expected for a melting snowpack in May in Utah.

3.2 Diurnal melt-freeze cycles in dielectric constant with time and depth

This study was conducted during the spring, where diurnal trends in daily temperatures often fluctuate above and below freezing during the day and night. For the May 19–May 22, 2013, period, the TDR probes remained in the snowpack for a few days. Figure 3.4 shows diurnal melt-freeze processes in the snowpack for three probe depths. These diurnal fluctuations in the snowpack dielectric constant are likely due to an increase in liquid water during the day as the snow melts and a decrease in the liquid water at night as the snow refreezes. On days when the difference between the minimum and maximum temperature is greatest, the fluctuation in the dielectric constant is also the

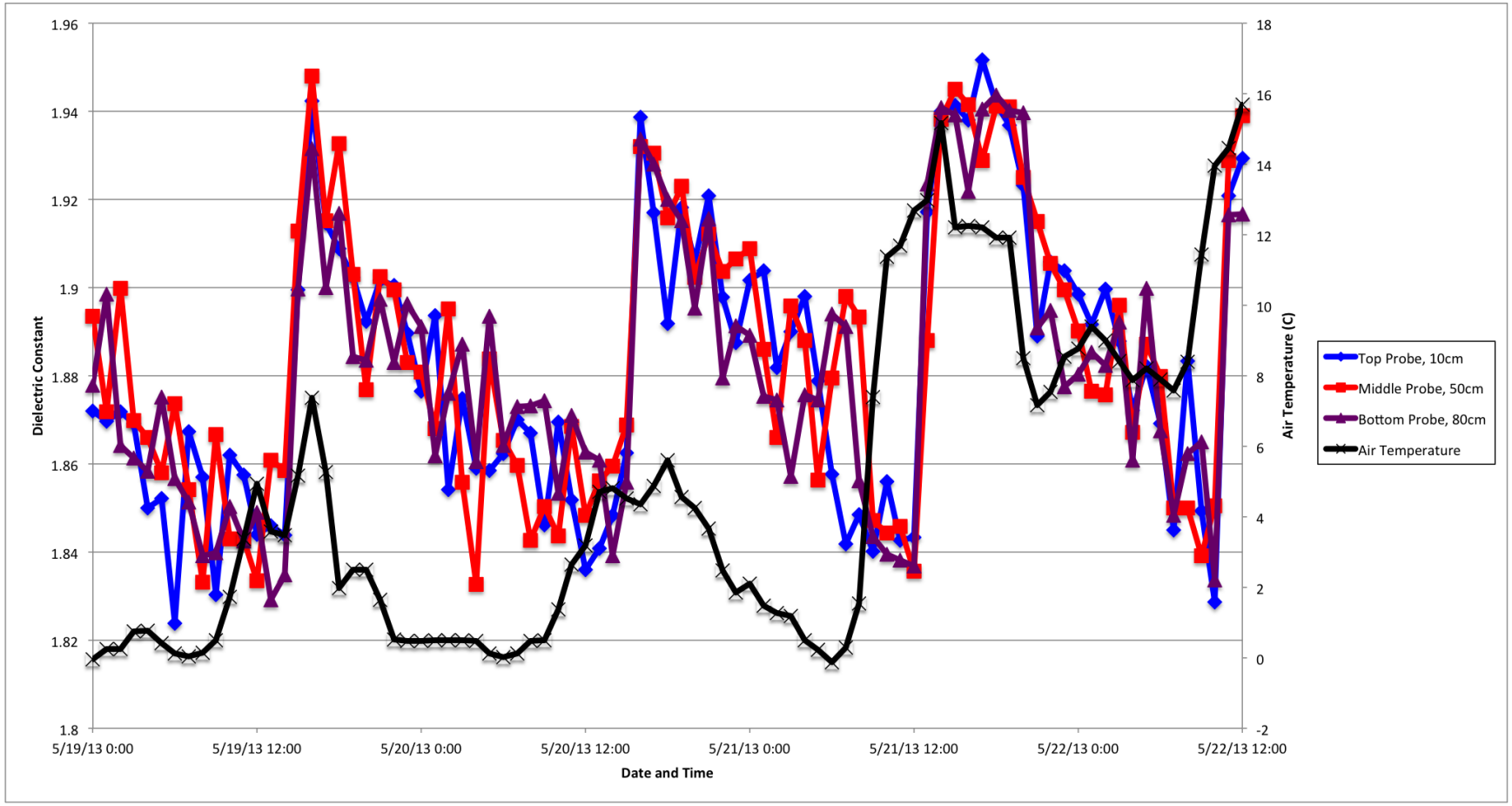

Figure 3.4: There are observable cycles in dielectric constant values measured with the TDR. When daytime temperatures exceed freezing and nighttime temperatures dip below freezing, diurnal fluctuations in measured dielectric values become more observable.

greatest as seen on May 21 and 22 in Figure 3.4. Air temperature and dielectric constant have the highest correlation for this period, which will be discussed in more detail in section 3.3.

This study did not find diurnal cycles in TDR measurements when the air temperature remained more than a couple of degrees above freezing for greater than 24-hour periods. Figure 3.5 shows an increasing dielectric constant over time, regardless of increased solar energy during the day or decreased air temperature at night. This increasing trend in the dielectric constant may be due to a constant presence of liquid water since air temperature did not drop below freezing, preventing the refreezing of snowpack layers (Figure 3.5).

According to Cagnati et al. (2004), during the night phase of diurnal melt-freeze cycles, the top 10 cm of the snowpack is often the greatest depth affected by nighttime refreezing. Analysis between the average daytime and average nighttime dielectric constant for May 19 through May 20, 2013, reveals that the top 10-cm probe refreezes more than the bottom probe at 80 cm with average dielectric constants of 1.863 and 1.872, respectively (Table 3.4). With TDR probe measurements, diurnal melt-freeze cycles are visible throughout the depth of the 80-cm sampled snowpack (Figure 3.4); however, the top and bottom probes are correlated with each other during the day (Figure 3.6) and are not correlated during the night (Figure 3.7). According to Techel and Pielmeier (2011), the uppermost layer of the snowpack is affected the most by daytime warming. Analysis of dielectric constant data reveals that all probe depths are affected by the diurnal cycle, and the top probe is more affected by the energy inputs received during the day than the 80-cm probe depth. Table 3.4 illustrates the stronger diurnal signal at the top of the

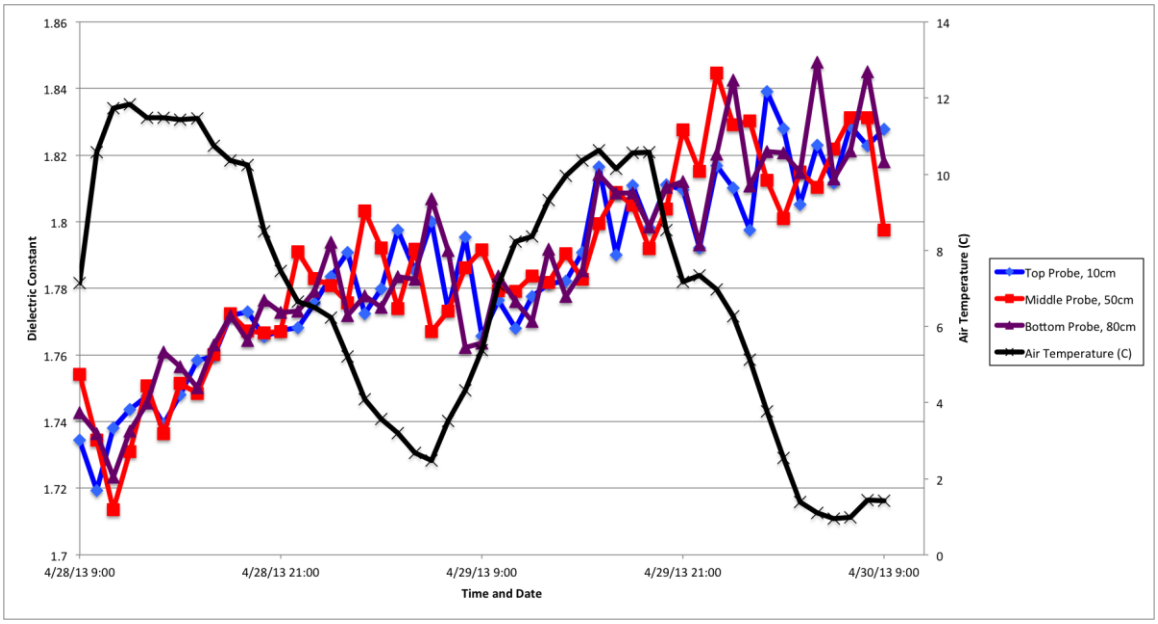

Figure 3.5: This figure shows a period from April 28 to April 30, 2013, where the air temperature remained above freezing. For this period, the dielectric constant is not dictated by melt-freeze cycles, melting controls the dielectric constant, which is indicated by the increasing dielectric constant.

Time period	Day-time	Night-time	Difference
Top Probe (10cm)	1.889	1.863	0.026
Bottom Probe (80cm)	1.884	1.872	0.012

Table 3.4: Average daytime and nighttime dielectric constant for the top and bottom probes form May 19–May 20, 2013.

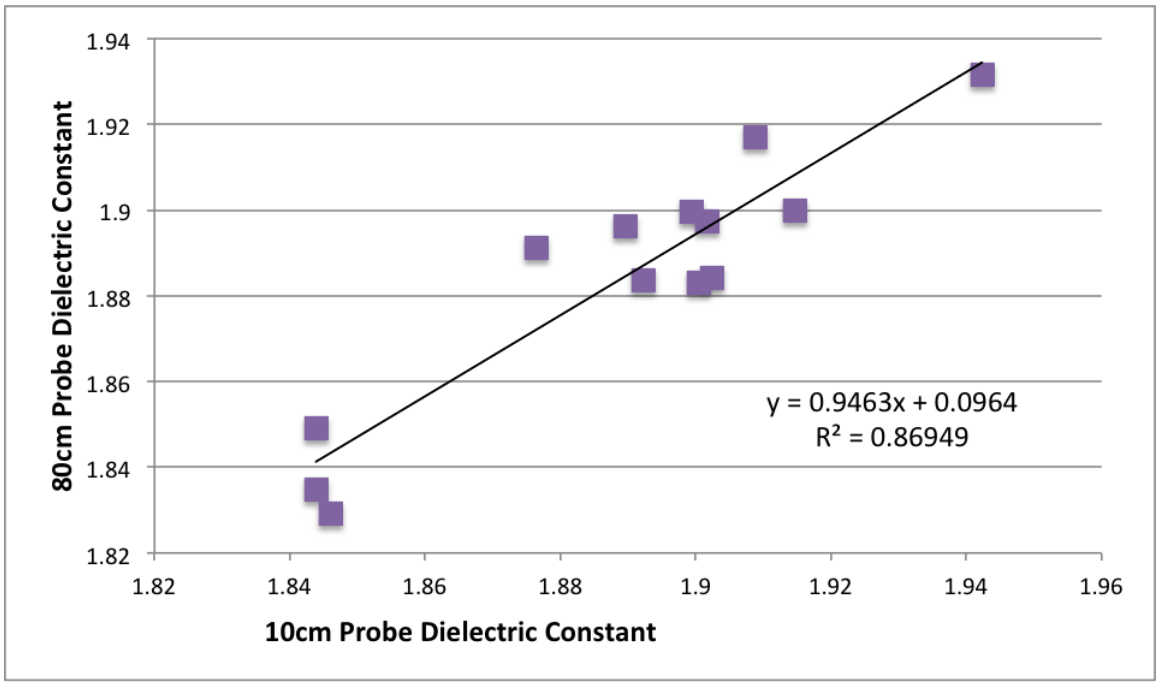

Figure 3.6: This graph shows higher daytime correlations on May 19, 2013.

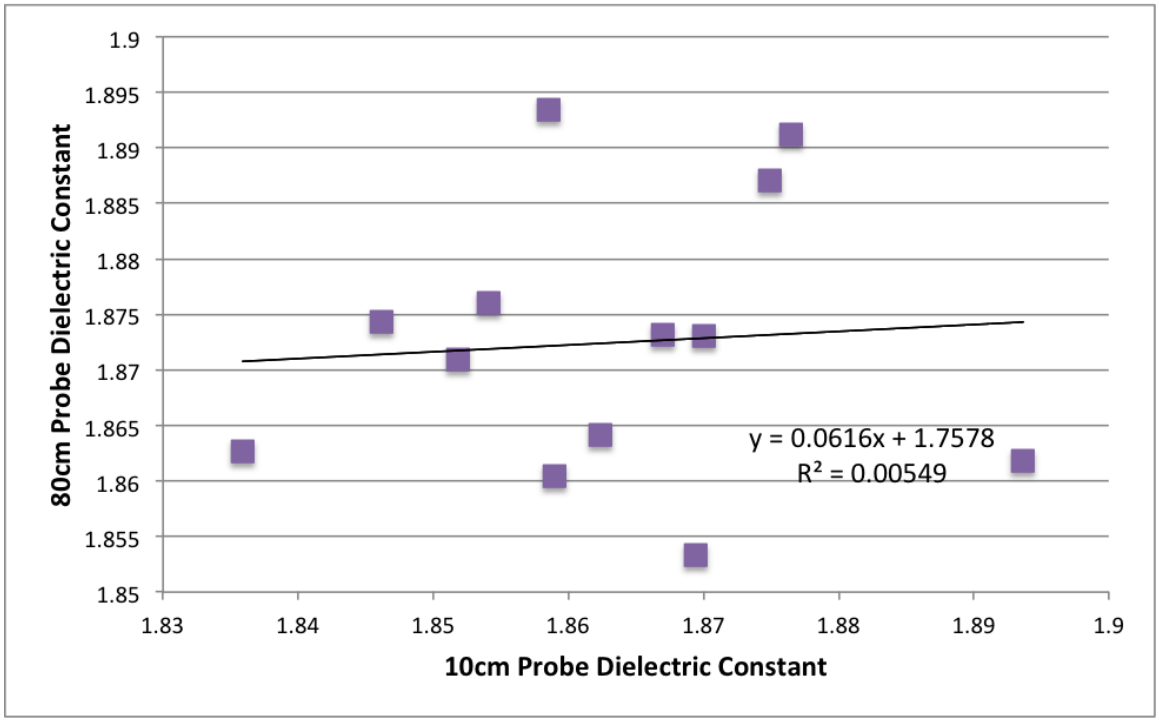

Figure 3.7: This graph shows almost no nighttime correlation from May 19–May 20, 2013.

snowpack with the top probe having over two times the difference between daytime and nighttime dielectric constants for this time period.

Figure 3.4 shows an increasing and decreasing dielectric value due to diurnal melt-freeze cycles. Correlation and offset between the top and all other probes was assessed. This analysis does not support the idea of a lag-time between the top probe and the bottom probe, as can be seen in Figures 3.8 and 3.9. Correlations between the top and bottom probes with no lag obtained an *r*-squared value of 0.697, while correlations between the top and bottom probes at a 1-hour lag obtained an *r*-squared value of 0.381. There are a few explanations for this–the time-step is too large to obtain an offset, or the offset is greater than 24 hours. Although diurnal cycles are visible at all probe depths, the data collected in this experiment limit further exploration of these ideas.

3.3 Correlation and lag in diurnal cycles between measured dielectric constant and energy received by the snowpack

This section assesses if and to what extent the dielectric constant values measured with the TDR are influenced by energy received by the snowpack, such as solar radiation and air temperature. The top probe at a depth of 10 cm was selected to correlate diurnal air temperature. Dielectric constant data were plotted with solar radiation data (Figure 3.10) and air temperature data (Figure 3.11) separately for May 19, 2013, through May 22, 2013. These plots show the measured snow dielectric constant following similar cycles in the measured dielectric constant with diurnal cycles in both solar radiation and diurnal cycles to both solar radiation and air temperature. Additionally, an offset can be seen between solar radiation and the dielectric constant and between air temperature and

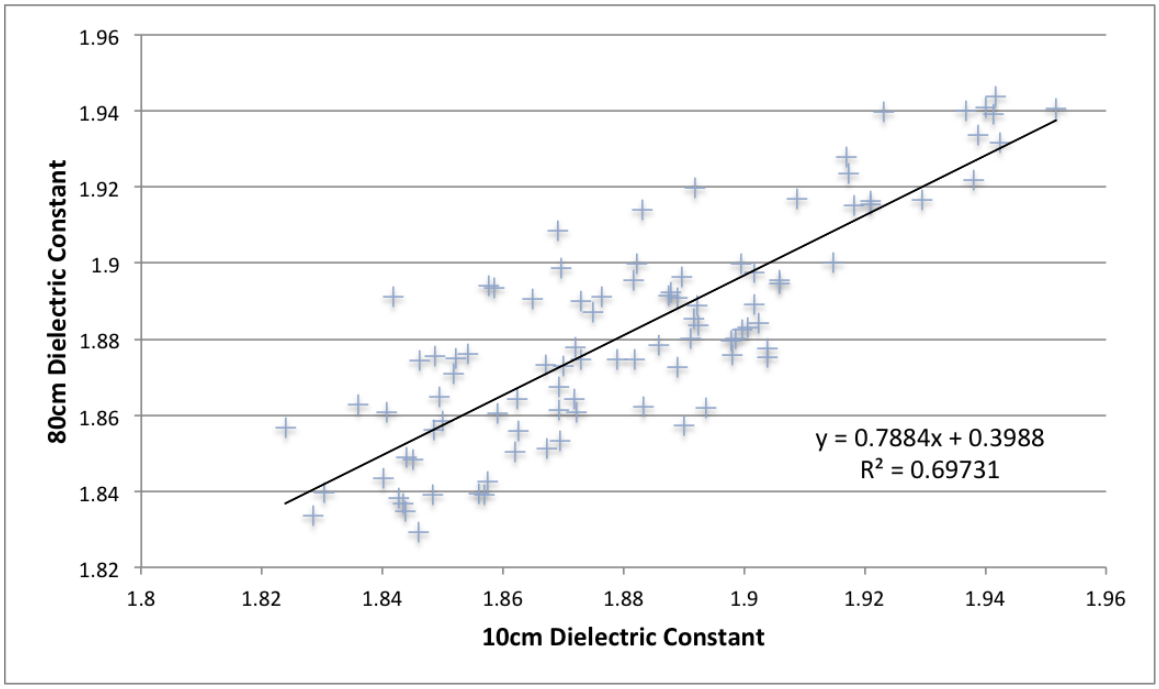

Figure 3.8: This graph shows higher correlations on May 19–May 21, 2013, with no lag between the top and bottom probes.

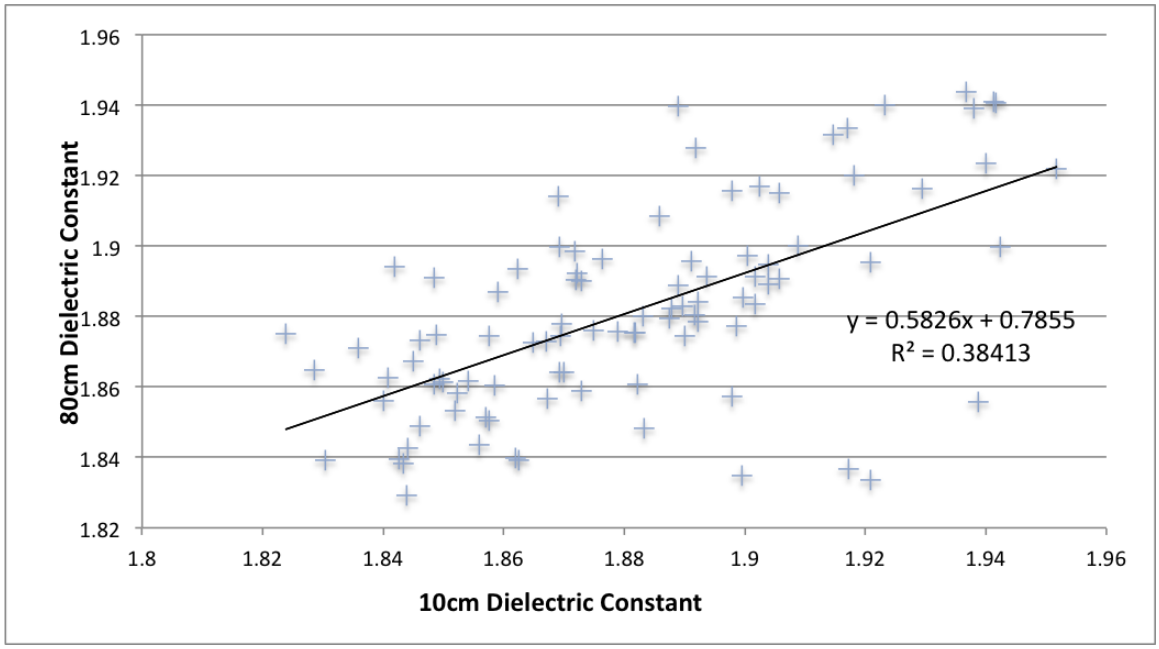

Figure 3.9: This graph shows lower correlations on May 19–May 21, 2013, with a 1-hour lag between the top and bottom probes.

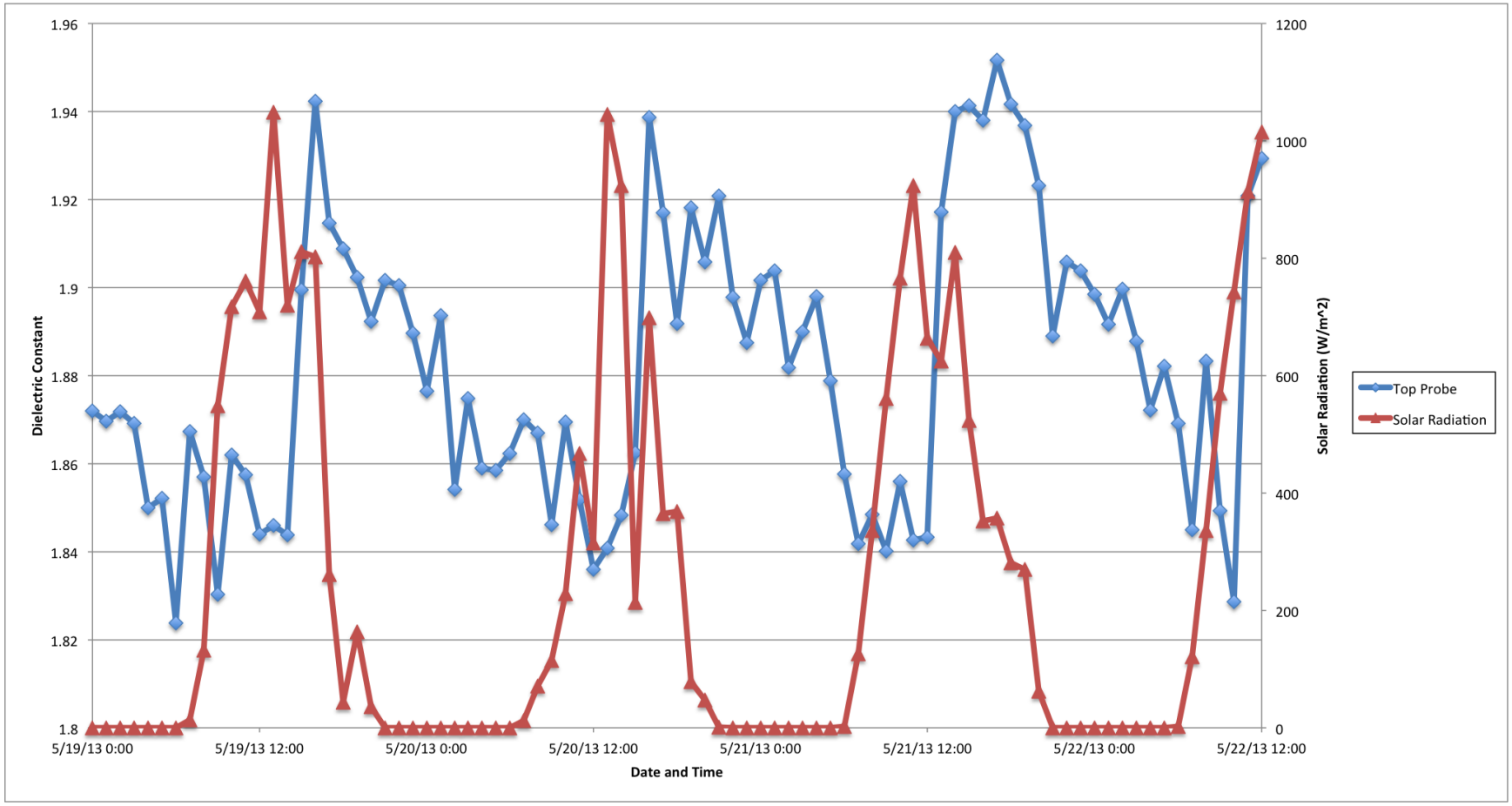

Figure 3.10: There are observable cycles in dielectric constant values measured with the TDR that coincide with diurnal solar radiation cycles. A lag in dielectric constant behind solar radiation, which will be quantified later in this section, is visible in this figure, especially around the peak solar radiation, which occurs at noon each day.

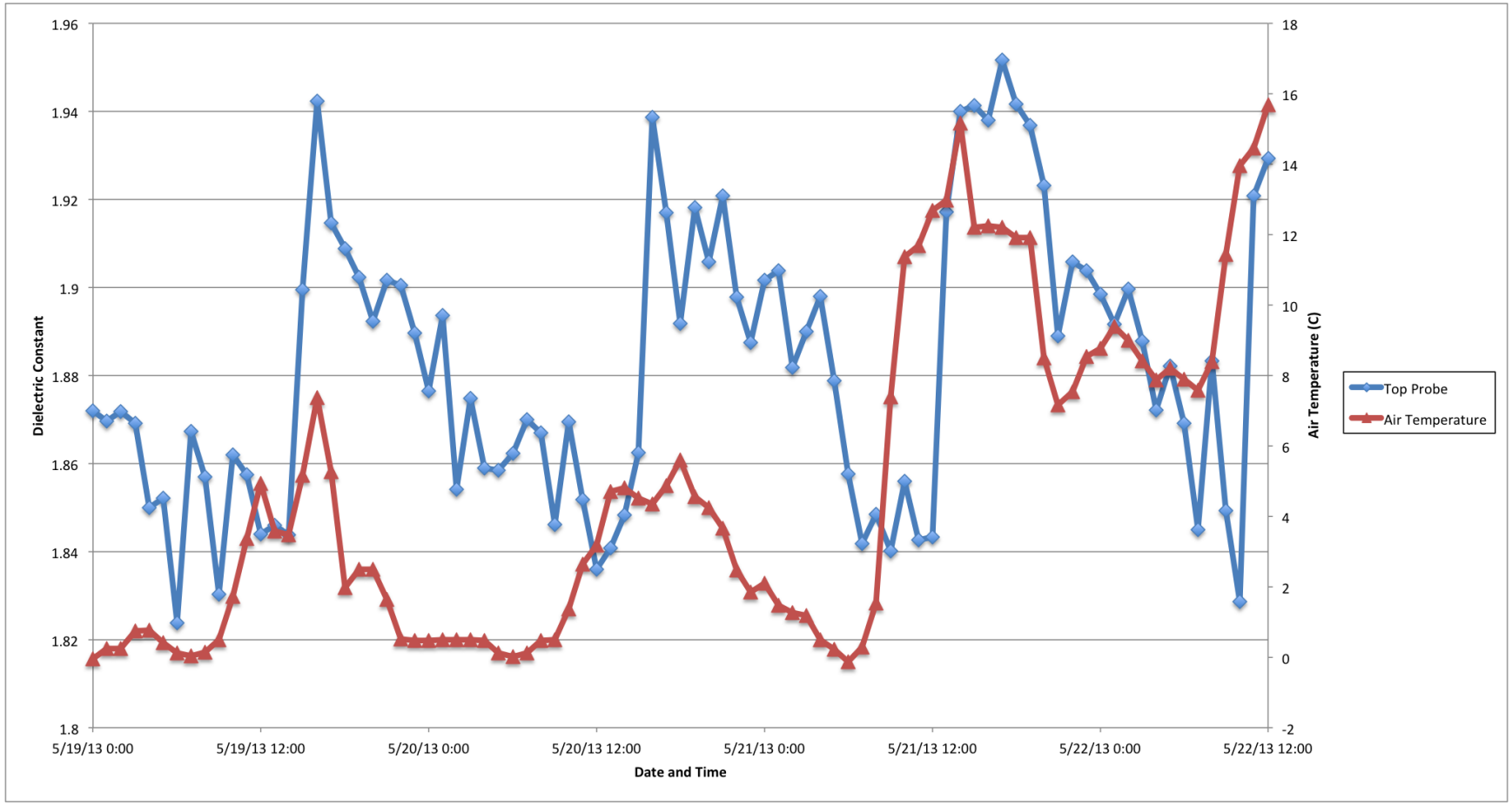

Figure 3.11: There are observable cycles in dielectric constant values measured with the TDR that coincide with diurnal air temperature cycles. When daytime temperatures exceed freezing and nighttime temperatures fall below freezing, diurnal fluctuations in measured dielectric values become more observable. On days when the temperature difference is greatest, the diurnal cycles of air temperature and dielectric value coincide best.

the dielectric constant. This is most evident in Figure 3.10 around noon on May 19 and May 20, 2013. An offset can also be seen in Figure 3.11 around noon on May 21, 2013. This section uses linear and multiple linear regression to quantify the lag and correlation between solar radiation, air temperature, and the dielectric constant for the period beginning at midnight on May 19 though midnight on May 22, 2013.

Linear regression was performed to understand the lag that exists between the energy inputs in the form of solar radiation and air temperature received by the snowpack and the snowpack's response to this energy increase through melting or response to the energy decrease through refreezing. Linear regression was performed for all possible midnight to midnight and noon to noon 24- and 48-hour time-periods between midnight on May 19 and midnight on May 22, 2013. Linear regression was assessed between solar radiation and the dielectric constant and between air temperature and dielectric constant for these time periods and at lags of 0 to 10 hours (Figure 3.12). Multiple linear regression between the dielectric constant and solar radiation and air temperature was assessed for all possible lag combinations between 0 and 10 hours for the time periods. Linear regression between solar radiation and air temperature at lags between 0 and 3 hours was assessed as well. The following sections discuss the results from this analysis. The highest correlation between solar radiation and dielectric constant for a 24-hour period was 0.705 with dielectric constant lagged 5 hours behind solar radiation and occurred from May 21 to May 22, 2013, from a midnight to midnight period (Figure 3.13). The highest correlation between solar radiation and dielectric constant for a 48-hour period was 0.582 with dielectric constant lagged 5 hours behind solar radiation and occurred from May 20 to May 22, 2013, from a midnight to midnight period (Figure

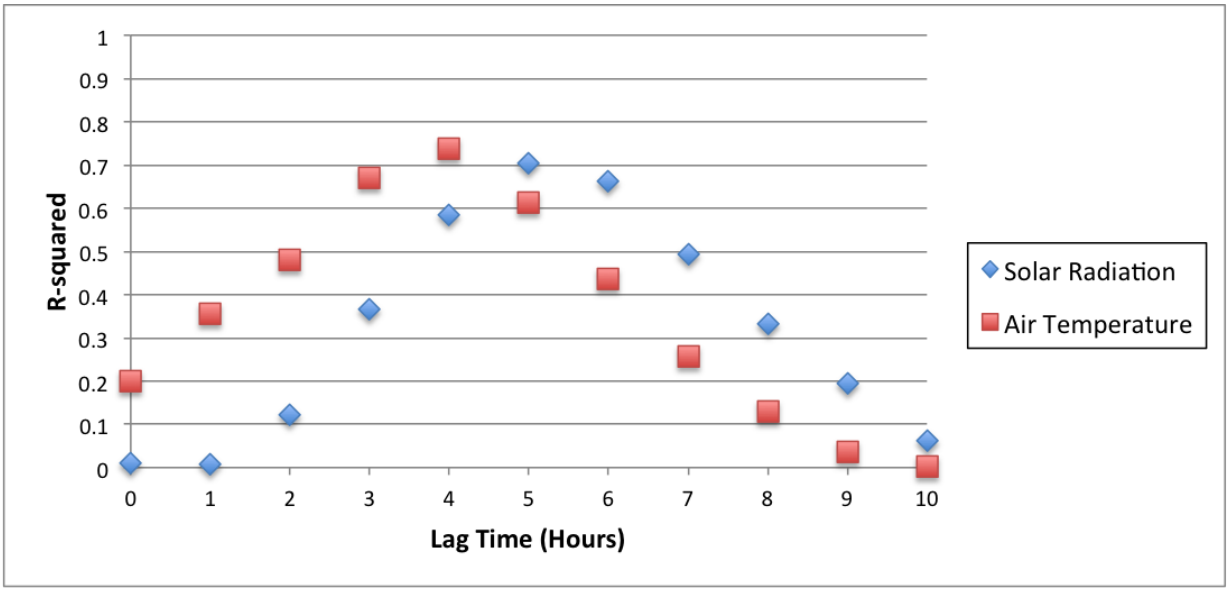

Figure 3.12: This figure shows the *r*-squared values between solar radiation and dielectric constant of the top probe and between air temperature and dielectric constant at lag-times of 0 to 10 hours for the May 21–May 22, 2013, 24-hour period.

3.14). The highest correlation between air temperature and dielectric constant for a 24-hour period was 0.737 with dielectric constant lagged 4 hours behind air temperature and occurred from May 21 to May 22, 2013, from a midnight to midnight period (Figure 3.15). The highest correlation between air temperature and the dielectric constant for a 48-hour period was 0.655 with the dielectric constant lagged 4 hours behind air temperature and occurred from May 20 to May 22, 2013, from a midnight to midnight period (Figure 3.16). Table 3.5 includes *r*-squared values for the time periods with the highest correlations at the associated lags.

Multiple linear regression between the dielectric constant, solar radiation, and air temperature was performed at all possible lag combinations between 0 and 5 hours for all 24- and 48-hour time periods between midnight on May 19 to midnight on May 22, 2013. The highest correlations were found with the dielectric constant lagged 5 hours behind

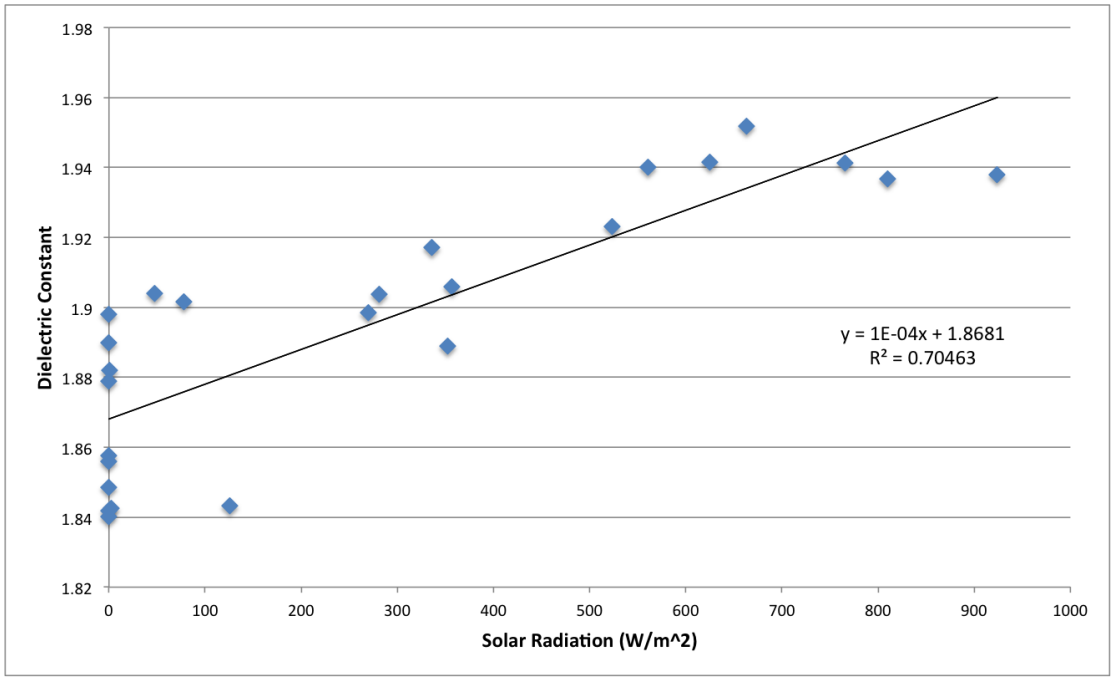

Figure 3.13: This figure shows the highest correlation and lag of 5 hours between solar radiation and dielectric constant for May 21–22, 2013, 24-hour time periods within the study period.

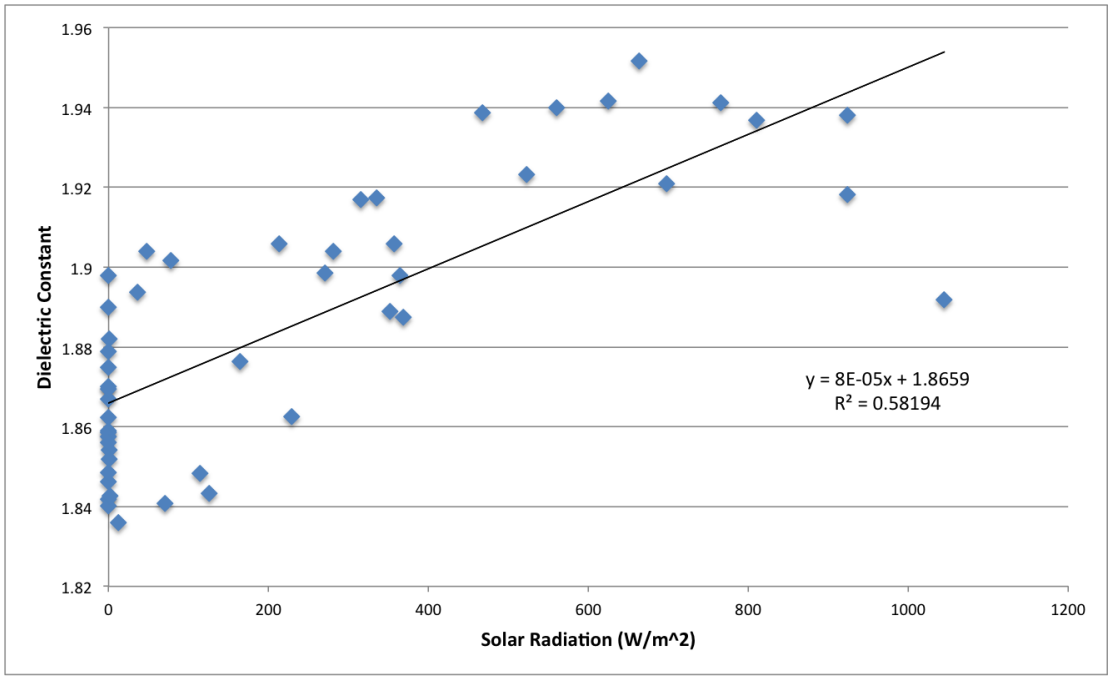

Figure 3.14: This figure shows the highest correlation and lag of 5 hours between solar radiation and dielectric constant from May 20–22, 2013 for 48-hour time periods within the study period.

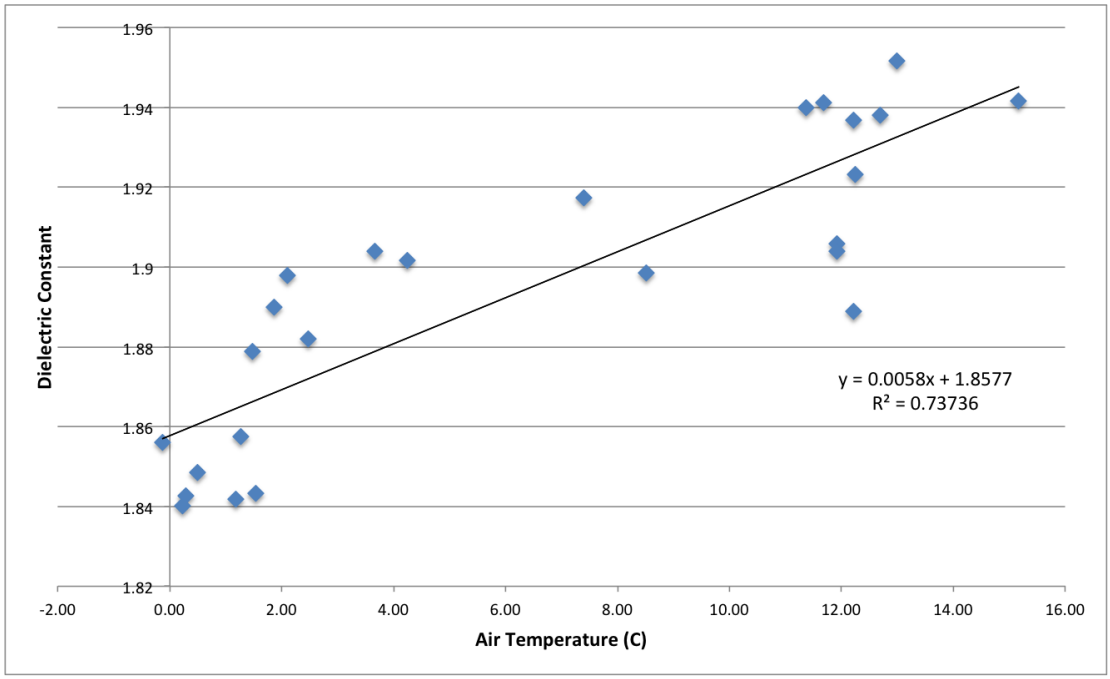

Figure 3.15: This figure shows the highest correlation and lag of 4 hours between air temperature and dielectric constant from May 21–22, 2013, for 24-hour time periods within the study period.

solar radiation and 4 hours behind air temperature for both 24- and 48-hours periods. The highest *r*-squared value found with multiple linear regression between the three variables for a 24-hour period was 0.763, and the highest correlation for a 48-hour periods was 0.714. These lag-times in the dielectric constant of 5 hours behind solar radiation and 4 hours behind air temperature found with multiple linear regression were consistent with the lag times for solar radiation and air temperature using simple linear regression.

Correlation between solar radiation and air temperature at lags of 0 through 3 hours were conducted. The highest correlation between solar radiation and air temperature for a 24-hour period was 0.862 with no lag in air temperature behind solar radiation and occurred from May 21 to May 22, 2013, from a noon to noon period (Figure 3.17). The highest correlation between solar radiation and air temperature for a

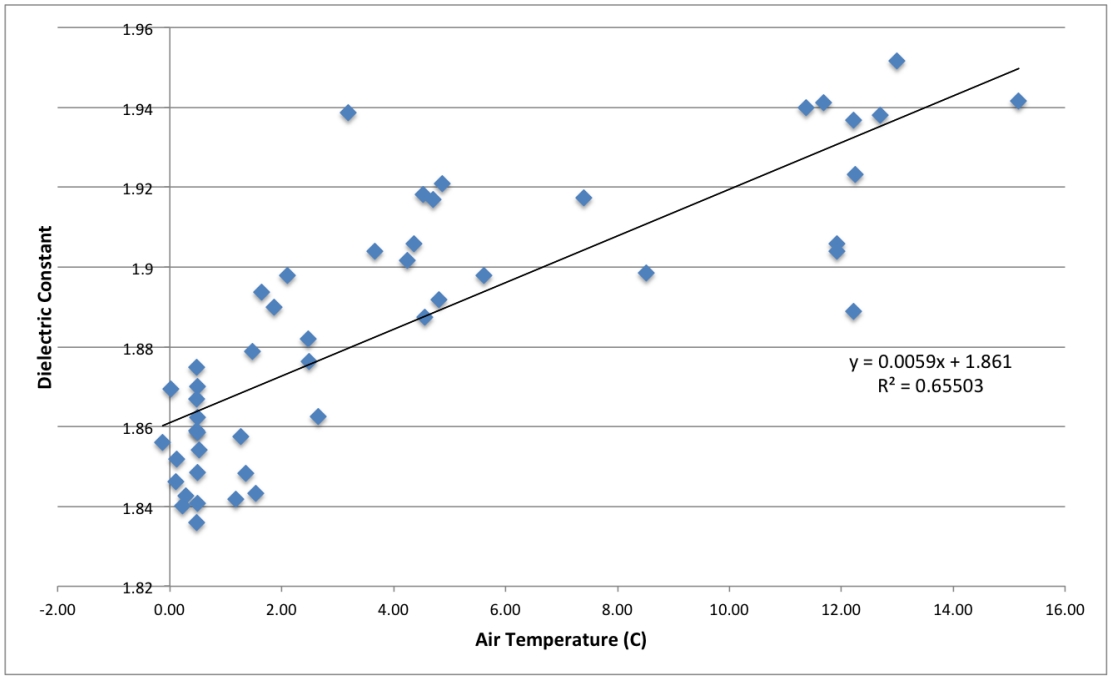

Figure 3.16: This figure shows the highest correlation and lag of 4 hours between air temperature and dielectric constant from May 20–22, 2013, for 48-hour time periods within the study period.

Table 3.5: This table shows the variables used in regression as well as the time period and dates on which the highest correlation was found. The *r*-squared values and lag times are also reported in this table.

Variables	**Time Period**	**Duration**	***R* squared**	Dates	**Lag**
Solar Radiation vs. Dielectric Constant	Midnight-Midnight	24	0.705	5/21–5/22	5
Solar Radiation vs. Dielectric Constant	Midnight-Midnight	48	0.582	5/20–5/22	5
Air Temperature vs. Dielectric Constant	Midnight-Midnight	24	0.737	5/21–5/22	4
Air Temperature vs. Dielectric Constant	Midnight-Midnight	48	0.655	5/20–5/22	4
Multiple Regression	Midnight-Midnight	24	0.763	5/21–5/22	5,4
Multiple Regression	Midnight-Midnight	48	0.714	5/20–5/22	5,4
Solar Radiation vs. Air Temperature	Noon-Noon	24	0.862	5/21–5/22	0
Solar Radiation vs. Air Temperature	Midnight-Midnight	48	0.600	5/19–5/21	1

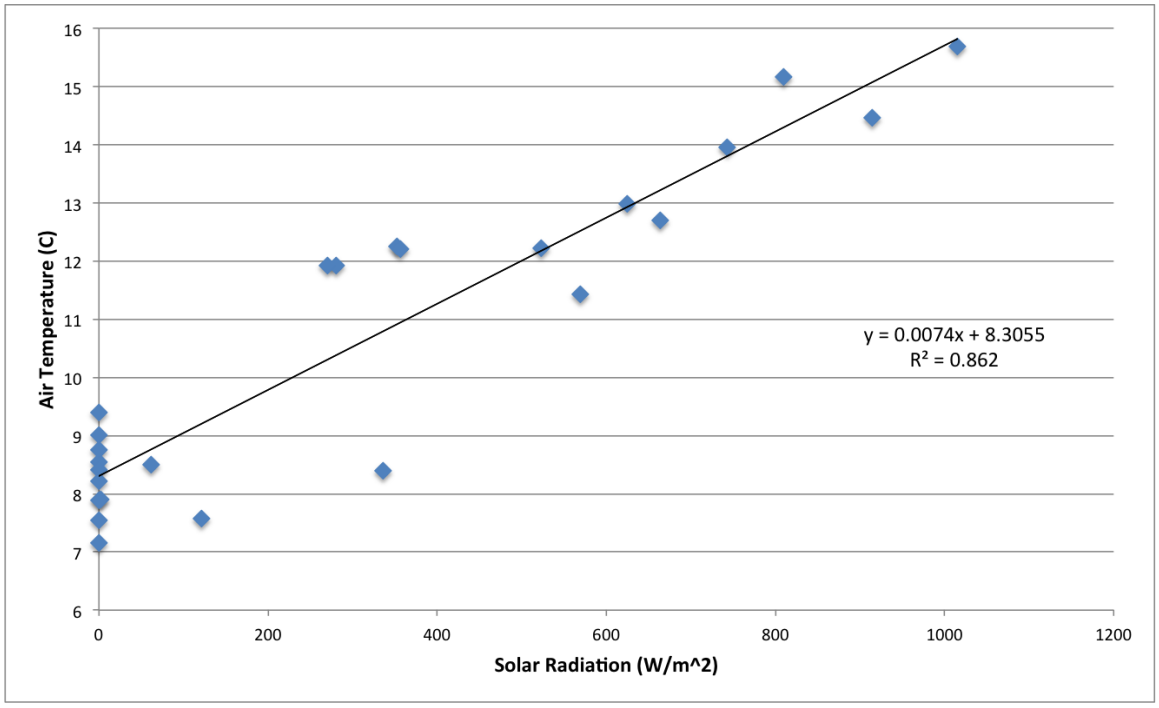

Figure 3.17: This figure shows the highest correlation and lag between solar radiation and air temperature for 24-hour time periods within the study period.

48-hour period was 0.6 with a 1-hour lag in air temperature behind solar radiation and occurred from May 19 to May 21, 2013, from a midnight to midnight period (Figure 3.18).

Results from linear regression and multiple linear regression suggest that this method could be used to establish a lag time between the energy from the sun or the overlying air mass received by the snowpack and the snowpack's conversion of this received energy into snowmelt or absence of energy into refreezing at night. In general the best correlation between variables occurred at midnight to midnight periods. This may be due to the time period beginning at the start of refreezing cycle and may not have much importance in the physical context of the snowpack. The highest correlation occurs at 24 hours, or shorter timescales, which could suggest that the snowpack reacts to energy inputs over a shorter time period during melting.

The highest correlation between solar radiation and the dielectric constant occurs with the dielectric constant lagged 5 hours behind solar radiation, while the highest correlation between air temperature and the dielectric constant occurs with the dielectric constant lagged 4 hours behind air temperature. When multiple regression is performed at all possible lag combinations between 0 and 5 hours with the dielectric constant lagging behind solar radiation and air temperature, the highest correlations for both 24- and 48-hour periods occurred with the dielectric constant lagged 5 hours behind solar radiation and 4 hours behind air temperature, which is consistent with the 5-and 4-hours lags found with linear regression of the dielectric constant and solar radiation and dielectric constant and air temperature.

Additionally, when linear regression is run between solar radiation and air

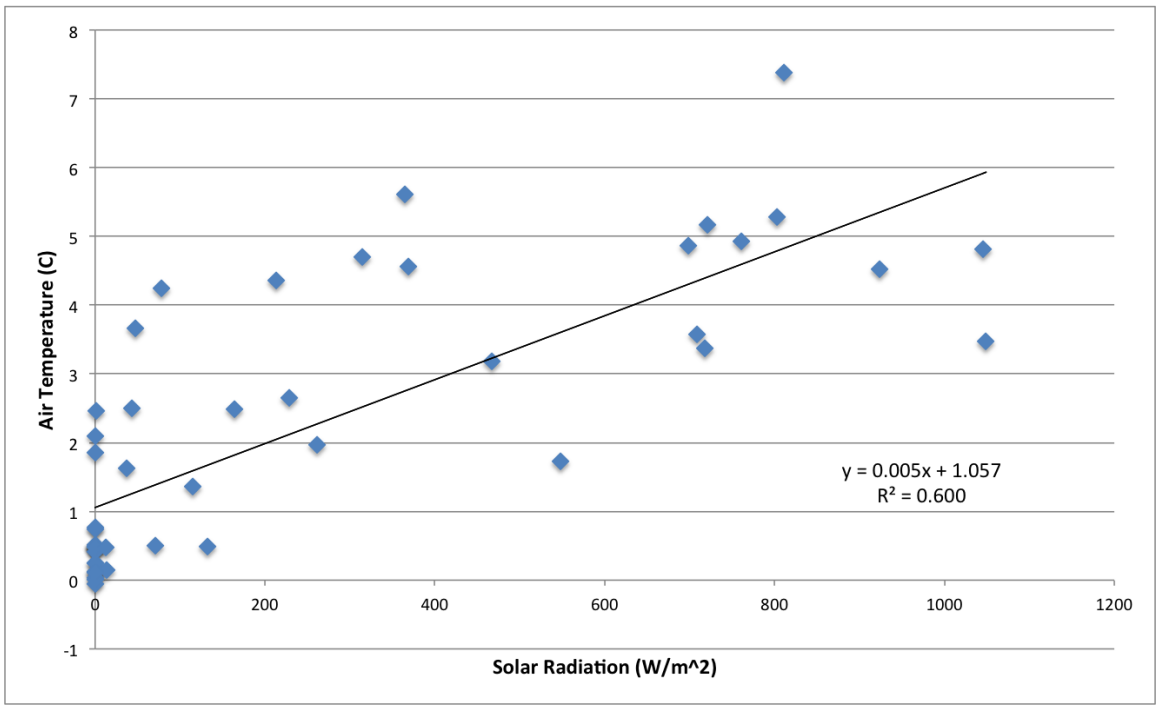

Figure 3.18: This figure shows the highest correlation and lag between solar radiation and air temperature for 48-hour time periods within the study period.

temperature at lags between 0 and 3 hours, the highest correlation is found when there is no lag between air temperature and solar radiation for a 24-hour time period and when air temperature lagged 1 hour behind solar radiation for a 48-hour time period. These differing lag times suggest that a time step shorter than 1 hour is needed to assess the lag between solar radiation and air temperature.

The consistency in the lag times for linear and multiple linear regression strengthen the concept that the energy inputs into the snowpack are not instantaneously converted to energy in the snowpack. The lag time of 5 hours for solar radiation in both linear and multiple linear regression suggest that the greatest lag time occurs when solar radiation is converted into energy in the snowpack. The lag time of 4 hours for air temperature as well as the lag in air temperature behind solar radiation suggests that air temperature lags behind solar radiation, which is commonly known in the physical

sciences (i.e., Huang et al., 2008; Prescott & Collins, 1951; Waldner et al., 2001). In addition, this suggests that the energy received by the snowpack from air temperature is more quickly converted into snowpack energy than the energy received from solar radiation.

Waldner et al. (2001) and Techel and Pielmeier (2011) noticed the dielectric constant and liquid water content fluctuations offset from daily solar radiation and air temperature fluctuations; however, they do not quantify this lag nor correlation. This study finds high correlation amongst solar radiation, air temperature, and the dielectric constant as well as consistent lag times. The analysis of correlation in diurnal melt-freeze cycles measured by the TDR to solar radiation and air temperature suggests that the TDR would be a good method for assessing energy inputs into the snowpack, and the delay is the snowpack's conversion of received energy into energy needed for snowmelt.

3.4 Snowpack liquid water content

This study recorded dielectric constant values for a wet snowpack during springtime snowmelt. According to Colbeck (1982), the permittivity will increase with increasing liquid water content. Liquid water content was calculated for all probe depths using Denoth's (1994) equation:

$$\varepsilon = 1 + 1.92\rho + 0.44\rho^2 + 0.187\theta + 0.0045\theta^2 \qquad (3.1)$$

Due to the nonlinearity of the equation and the lower density values used to calculate the offset, it was found that when the snow density exceeds 420kg/m^3, with the dielectric constants recorded by the probe adjusted with the offset, the resulting liquid water content could not be found. This issue may arise from the calculation of the offset since only dry snow densities between 200 and 400 kg/m^3 were available to calculate the offset.

Perhaps a greater offset of the dielectric constant for snow densities over 400kg/m^3 is needed to accurately assess liquid water content in these more dense layers. This limited the probe depths that liquid water content could be studied to the probes at 10-cm, 20-cm, and 40-cm depths. Even with this limitation, interesting findings were revealed in this study.

Liquid water content remained the highest at the top of the snowpack for the period May 19 at midnight to May 22 at noon. Diurnal cycles that coincide with solar radiation and air temperature cycles are apparent in this data. Figure 3.19 shows these diurnal cycles of liquid water content in the 10-cm, 20-cm, and 40-cm probes with air temperature and liquid water content**.** In addition, the three probes with liquid water content values follow a similar cyclical pattern. The hypothesis for the downward propagation of liquid water is that as wetness increases in the snowpack, liquid water will begin to propagate downward. On average the 10-cm probe has the greatest liquid water content of 2.39 vol. %, the 40-cm probe has the lowest liquid water content of 1.46 vol. %, with the average liquid water content of 1.72 vol. % for the 20-cm probe falling between these two values for the time period (Table 3.6). Perhaps the hypothesis would be more accurate for a study that measures the dielectric constant for the entire snowmelt period. In addition, a greater depth may be needed to assess the downward propagation of liquid water since the water may drain from the top of the snowpack more quickly and become pooled in the bottom of the snowpack or in layers below the measured 40 cm. The use of 5-cm staggered probe spacing may be able to capture the movement of the wetting front through the snowpack (Lundberg, 1997).

Denoth found greater liquid water content at the top of the snowpack than at a 40-

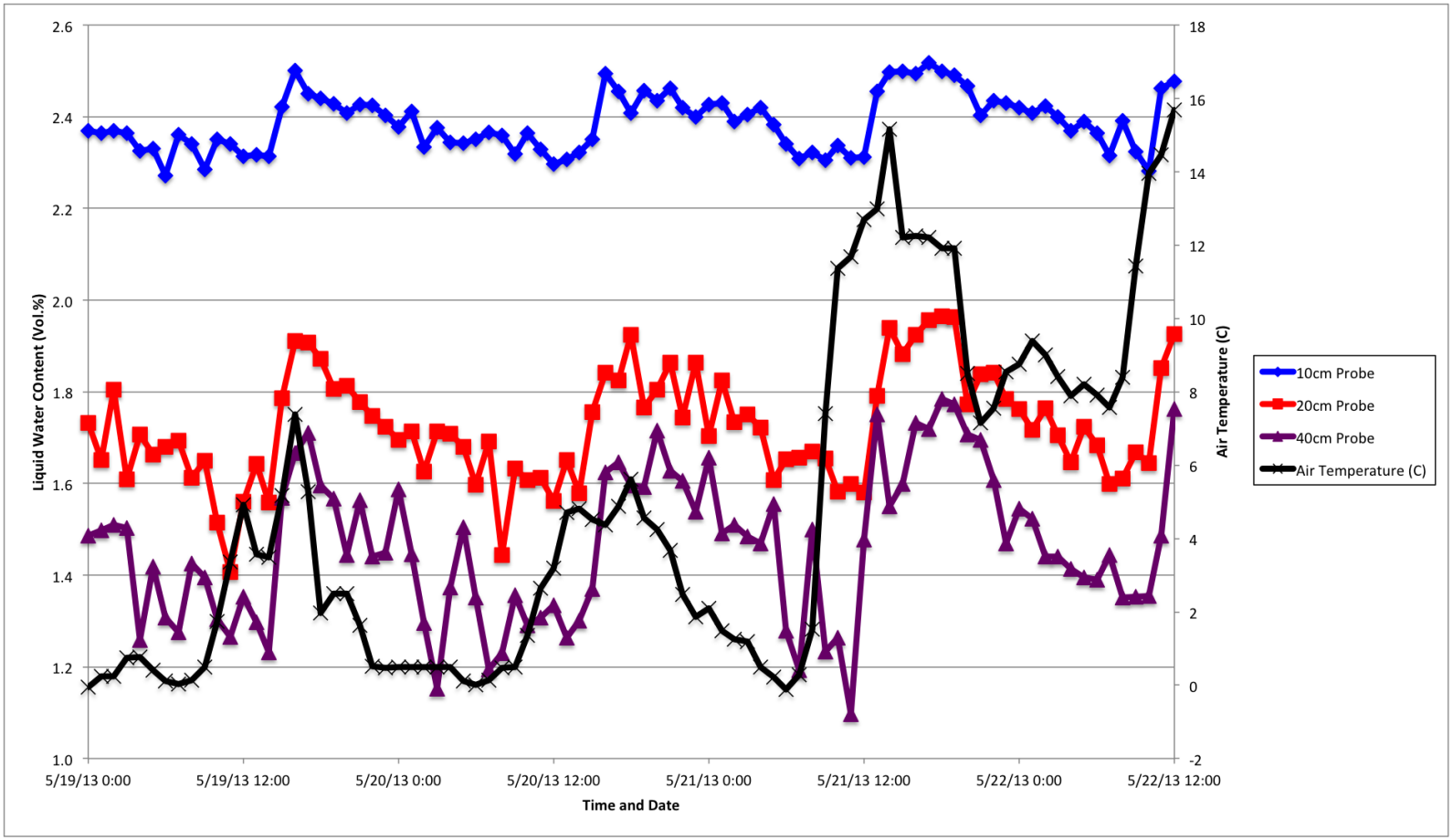

Figure 3.19: This figure shows diurnal cycles in liquid water content recorded by the 10-cm, 20-cm, and 40-cm probes that coincide with diurnal cycles in air temperature.

Table 3.6: Average daytime and nighttime dielectric constant for the top and bottom probes form May 19–May 20, 2013.

	10cm Probe	20cm Probe	40cm Probe
Average (vol.%)	2.386	1.720	1.463
Max (vol.%)	2.518	1.965	1.784
Min (vol.%)	2.272	1.406	1.096
Difference (vol.%)	0.246	0.559	0.688

cm depth using a capacitance sensor (Denoth, 1994). Denoth noted that the wetness at the 40-cm depth fluctuated from 1.0 vol. % to 1.5 vol. %. My results for the 40-cm probe depth were fairly similar with fluctuations from 1.1 vol. % to 1.8 vol. %. This suggests that the probes work well at quantifying liquid water content in the top 40 cm of the snowpack.

The results obtained from this portion of the study are very similar to results from Waldner (2001) with higher liquid water content in the top probe than in the lower probe. Figures 3.20a and 3.20b show the diurnal cycles in the 10-cm, 20-cm, and 40-cm probe depths alongside diurnal cycles in air temperature and solar radiation for the same period. These finding are consistent with other studies that have found higher liquid water content in the top of the snowpack (i.e., Denoth, 1994; Techel & Pielmeier, 2011). Physical processes that act on the snowpack explain this greater liquid water content at the top of the snowpack. Solar radiation and air temperatures will have a greater impact at the top of the snowpack since the upper layers of the snow act as insulators to lower snowpack depths. This will cause the upper layers of the snow to become wetter sooner and retain additional liquid water.

3.5 Discussion of study in context of prior research and suggested improvements to current study

In Waldner et al. (2001) with a capacitance sensor and Stacheder (2005) with a Snowpower Band and TDR both used to measure snowpack dielectric constant, fluctuations in the dielectric constant were attributed to daily melt-freeze cycles. Data collected for this study during periods when nighttime temperatures were below freezing

a)

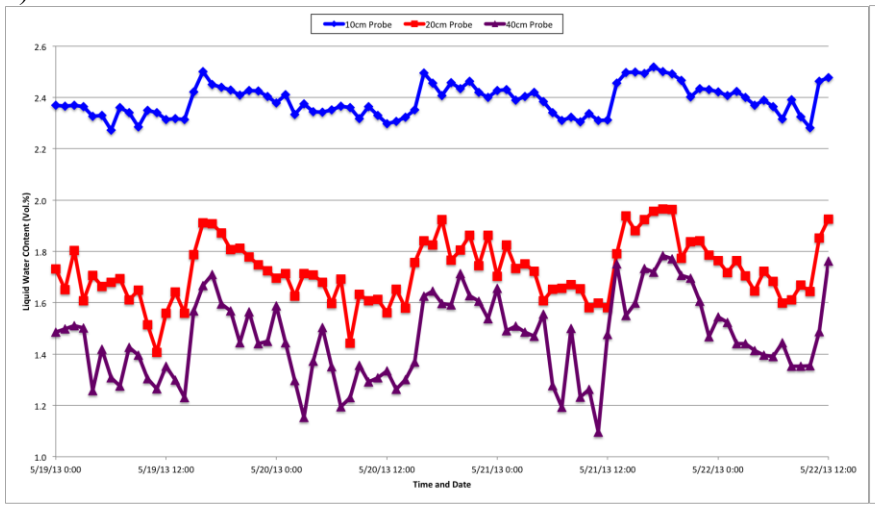

b)

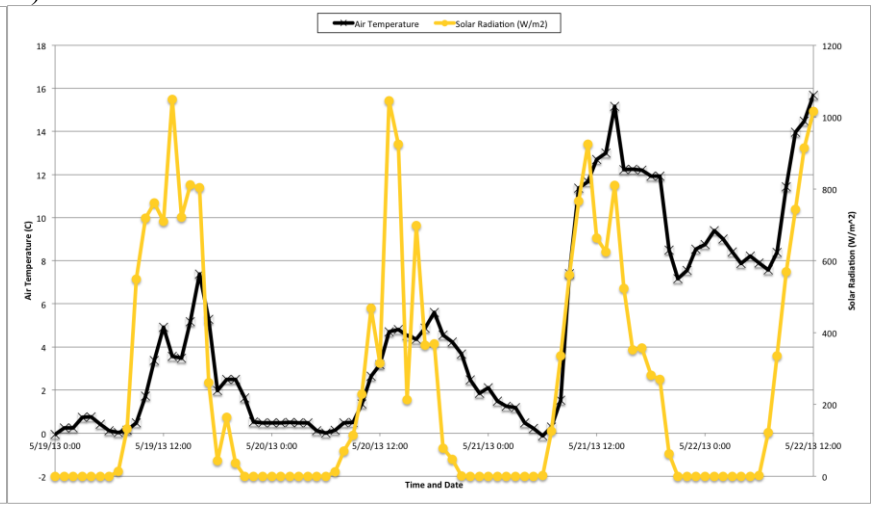

Figure 3.20: These figures are very similar to the figures produced in Waldner (2001). Liquid water content measured at 10 cm, 20 cm, and 40 cm is shown in Figure 3.20 (a). Solar radiation and air temperature are shown in Figure 3.20 (b) for the May 19 to 22, 2013, time period.

and daytime temperatures exceeded freezing show a similar trend of increased dielectric constant values during the day, indicating melting and decreased dielectric constant values at night, indicating refreezing. Future work to better assess if there are trends in the strength of diurnal fluctuations in the dielectric constant could use multiple probes to measure the dielectric constant within each homogeneous layer to better capture variability within each snowpack layer.

This study shows the TDR method with probes' applicability to both qualitatively and quantitatively track fluctuations in the daytime melting and nighttime refreezing of the snowpack due to fluctuations in snowpack liquid water content. In Stacheder (2005), an increasing dielectric constant was observed during springtime melting. This study observed a similar trend of increasing dielectric due to melting with a TDR placed throughout the top 80 cm of the snowpack when air temperature remained above freezing throughout an entire 24-hour period. Perhaps if probes were placed throughout the entire depth of the snowpack, instead of the top 80 cm, a downward propagation of liquid water through downward increases in dielectric constant would be able to be observed.

Waldner et al. (2001) found diurnal melt-freeze cycles with their horizontal band implementation and also noted that an increase in air temperature above 0 °C forces melting, especially in the uppermost layers. Techel and Pielmeir (2011) also found increased snow wetness in the uppermost 10 cm of the snowpack with the Snow Fork, Denoth meter, and hand squeeze test, which they contributed to daytime warming. Linear regression and analysis of the probe dielectric constant indicate daytime energy inputs into the snowpack increase the snowpack liquid water content more readily in the uppermost layers of the snowpack. Waldner et al. uses Snowpower Bands to observe that

the dielectric constant is lagged behind solar radiation and air temperature, but does not quantify the lag nor the correlation as done here. This study uses linear and multiple linear regression to correlate the measured dielectric constant to solar radiation and air temperature to find the highest correlation amongst these variables and the lag-time in the dielectric's response to solar radiation and air temperature. Consistent lag-times obtained with this study suggest that the TDR could be used in the future to assess how factors that influence energy fluxes, such as soil temperature and rain events, act within the snowpack. Additional work could be done to assess the quantity of solar radiation and other energy budget parameters and the response of the dielectric constant in both dry and wet snow.

Calculations of liquid water content with the TDR and probe result in fairly similar liquid water content calculations to Denoth (1994). The uppermost probe recorded the highest liquid water content, while the 40-cm probe measured the lowest liquid water content. In addition to previous studies that suggest the uppermost 10 cm of the snowpack contains the greatest liquid water, physical processes support this idea. The uppermost layer of the snow is closest to the overlying air mass and will therefore exchange more energy with the air mass than the lower snowpack layers. In addition, this uppermost layer is directly absorbing solar radiation, while lower layers receive solar radiation that has passed through upper snowpack layers and been transferred downward and throughout the snowpack.

CHAPTER 4

CONCLUSION AND RECOMENDATIONS FOR FUTURE WORK

Snowpack properties, such as SWE, density, and liquid water content, are important characteristics for predicting springtime flooding, domestic and agricultural water supply, hydropower planning, and avalanche forecasting. This study used manual density measurements as well as automated dielectric constant measurements with TDR in order to better understand the relationships amongst snow density, liquid water content, dielectric constant, and energy inputs into the snowpack and the applicability of TDR dielectric constant measurements to measure diurnal melt-freeze cycles and liquid water content in the snowpack layers.

This study shows that TDR probes measuring dielectric constant and manual density measurements are able to calculate an offset that can be applied to dielectric constants obtained for wet snow with the same system to compute snow wetness values. With improvements in TDR and probe calibration, the TDR and probe method may be able to produce automated density estimates without the need to use a snow cutter and scale. This can provide a better understanding of the temporal evolution of snowpack density and may have implications for both avalanche forecasters and snow hydrologists.

Variations in the dielectric constant, responding to diurnal melt-freeze cycles, driven by daytime solar radiation and warming are recorded by the TDR. Correlation and

lag-time amongst dielectric constant, solar radiation, and air temperature as well as correlation between probes at different depths suggests the melting and freezing recorded by the TDR and probe method is spurred by daytime energy inputs. Increased liquid water in the uppermost snowpack layers has been noted in several studies and was found in this TDR study. Different experimental designs utilizing multiple probes and more accurately assessing the energy inputs into the snowpack could be used to further study how energy received by the snowpack directly affects snowpack liquid water content and density.

Qualitative information on increasing and decreasing the dielectric constant from TDR probe measurements can be used to help more accurately forecast the likelihood of wet avalanches as well as the onset of peak flow in streams due to snowpack melt. Further research needs to be conducted into the applicability of TDR for monitoring long-term snowpack evolution. If the snowpack is able to heal air holes formed around probes, which occurred in this study, then probes could be installed in snowpacks to continuously measure fluctuations in the dielectric constant that can then be attributed to fluctuations in density due to compaction and melt-freeze cycles as well as increased liquid water content due to melting. This project advances scientists' understanding of how the electrical properties of snow can be used to understand the snow's physical processes.

APPENDIX A

TOPP'S RELATIONSHIP

Topp's Relationship describes the relationship between volumetric water content of soil and its dielectric constant. This is an empirical relationship, which uses both polynomial and linear forms. Topp's equation for volumetric water content, θ_v, is as follows:

$$\theta_v = -5.3 * 10^{-2} + 2.92 * 10^{-2} K_a - 5.5 * 10^{-4} K_a^2 + 4.3 * 10^{-6} K_a^3 \text{ [B.1].}$$

(TDR 100 manual, 2010)

APPENDIX B

FREEZING CALORIMETRY

Freezing calorimetry is the amount of heat released when ice goes from a solid state to water, a liquid state. The theory behind freezing calorimetry is a simple heat transfer equation. In order to calculate liquid water content from freezing calorimetry, a snow sample with a known mass and temperature is added to a calorimeter, which contains a known mass of a liquid freezing agent. Temperature is recorded before and after the liquid water in the snow sample freezes. The procedure consists of agitating the snow/freezing agent mixture until the sample becomes frozen and reaches an equilibrium temperature. The amount of water in the snow sample can be calculated since both the heath capacities of the freezing agent and water as well as the latent heat of fusion of water are known (Austin, 1990).

APPENDIX C

DILUTION METHOD

The dilution method is a technique used to quickly assess the liquid water content in the snowpack. According to Davis et al. (1985), the dilution method consists of an aqueous solution, which is diluted by the wet snow. The concentration change from before the aqueous solution is added and after wet snow is added forms the basis for the measurement.

REFERENCES

Ambach, W., & Denoth, A. (1972). Studies on the dielectric properties of snow. *Zeitschrift für Gletscherkunde und Glazialgeologie*, *8*, 113–123.

Assaf, H. (2007). Development of an energy-budget snowmelt updating model for incorporating feedback from snow course survey measurements. *Journal of Engineering, Computing and Architecture*, *1*(1).

Austin, R. T. (1990). *Determination of the liquid water content of snow by freezing calorimetry.* Ann Arbor, MI: University of Michigan, Department of Electrical Engineering and Computer Science.

Baggi, S., & Schweizer, J. (2009). Characteristics of wet-snow avalanche activity: 20 years of observations from a high alpine valley (Dischma, Switzerland). *Natural Hazards*, *50*(1), 97–108.

Cagnati, A., Crepaz, A., Macelloni, G., Pampaloni, P., Ranzi, R., Tedesco, M., ...Valt, M. (2004). Study of the snow melt-freeze cycle using multi-sensor data and snow modelling. *Journal of Glaciology*, *50*(170), 419–426.

Campbell, F., Nienow, P., & Purves, R. (2005). *Role of a supraglacial snowpack in mediating the delivery of meltwater to the glacier system: implications for glacier dynamics*. In Proceedings of the Annual Meeting-Eastern Snow Conference, Waterloo, ON, Canada (Vol. 62 pp. 193–207).

Campbell Scientific, Inc. (2010). *TDR100 instruction manual*. Logan, UT: Author.

Colbeck, S. C. (1982). The geometry and permittivity of snow at high frequencies. *Journal of Applied Physics*, *53*(6), 4495–4500.

Coléou, C. (1998). *Compte-rendu des essais de mesures de Densites et de Teneurs en Eau Liquide (T.E.L) de la Neige a l'aide d'une method de Reflectometrie dans le Somaine Temporel (T.D.R.)*, Laboratory Report. Grenoble, France: Centre d'Etudes de la Neige.

Cumming, W.A. (1952). The dielectric properties of ice and snow at 3.2 centimeters, *Journal of Applied Physics*, *23*(7), 768–773.

Davis, R. E., Dozier, J. LaChapelle, E. R., & Perla, R. (1985). Field and laboratory measurements of snow liquid water by dilution. *Water Resources Research*, *21*(9), 1415–1420.

Dielectric constant. (2012). *Britannica Online Academic Edition, Britannica online academic edition*. Retrieved from http://sfxhosted.exlibrisgroup.com/

Doesken, N. J., & Judson, A. (1997). *The snow booklet: A guide to the science, climatology, and measurement of snow in the United States.* Retrieved from http://ccc.atmos.colostate.edu/pdfs/snowbook.pdf

Frolov, A., & Macheret, Y. (1999). On dielectric properties of dry and wet snow. *Hydrological Processes*, *13*, 1755–1760.

Harper, J. T., & Bradford, J. H. (2003). Snow stratigraphy over a uniform depositional surface: Spatial variability and measurement tools. *Cold Regions Science and Technology*, *37*(3), 289–298.

Huang, S., Rich, P. M., Crabtree, R. L., Potter, C. S., & Fu, P. (2008). Modeling monthly near-surface air temperature from solar radiation and lapse rate: Application over complex terrain in Yellowstone National Park. *Physical Geography*, *29*(2), 158–178.

Johnson, J. B., & Schaefer, G. L. (2002). The influence of thermal, hydrologic, and snow deformation mechanisms on snow water equivalent pressure sensor accuracy. *Hydrological Processes*, *16*(18), 3529–3542.

Julander, R. (n.d.). *Snow hydrology: Importance of snow*. Informally published manuscript, Civil Engineering, University of Utah, Salt Lake City, UT. Retrieved from http://www.civil.utah.edu/~cv5450/intro.html.

Katsushima, T., Yamaguchi, S., Kumakura, T., & Sato, A. (2013). Experimental analysis of preferential flow in dry snowpack. *Cold Regions Science and Technology*, *85*, 206–216.

Kattelmann, R. C. (1985). Macropores in snowpacks of Sierra Nevada. *Annals of Glaciology*, *6*, 272–273.

Lee, J. H., & Wang, W. (2009). Characterization of snow cover using ground penetrating radar for vehicle trafficability—Experiments and modeling. *Journal of Terramechanics*, *46*(4), 189–202.

Linde, J., & Grab, S. (2011). The changing trajectory of snow mapping. *Progress in Physical Geography*, *35*(2), 139–160.

Looyenga, H. (1965). Dielectric constants of homogeneous mixture. *Molecular Physics*,

9(6), 501–511.

Lundberg, A. (1997). Laboratory calibration of TDR-probes for snow wetness measurements. *Cold Regions Science and Technology*, *25*(3), 197–205.

Lundberg, A., Granlund, N., & Gustafsson, D. (2010). Towards automated 'Ground truth'snow measurements–A review of operational and new measurement methods for Sweden, Norway, and Finland. *Hydrological processes*, *24*(14), 1955–1970.

Mätzler, C. (1996). Microwave permittivity of dry snow, *IEEE Transactions on Geoscience and Remote Sensing*, *34*, 573–581.

Niang, M., Bernier, M., Van Bochove, E., & Durand, Y. (2006). Precision of estimated Snow Water Equivalent (SWE) derived from the new sensor SNOWPOWER in Quebec (Canada). *Houille Blanche, 2*, 128–133.

Noborio, K. (2001). Measurement of soil water content and electrical conductivity by time domain reflectometry: A review. *Computers and Electronics in Agriculture*, *31*(3), 213–237.

Pielmeier, C. (2003). Textural and mechanical variability of mountain snowpacks (Doctoral Dissertation). University of Bern, Switzerland. Retrieved from http://fsavalanche.com

Prescott, J. A., & Collins, J. A. (1951). The lag of temperature behind solar radiation. *Quarterly Journal of the Royal Meteorological Society*, *77*(331), 121–126.

Rikkers, M. (n.d.). *Dielectric Constant*. Informally published manuscript, Civil Engineering, University of Utah, Salt Lake City, UT. Retrieved from http://www.civil.utah.edu/~cv5450/dielectric_const.html.

Ryan, W. A., Doesken, N. J., & Fassnacht, S. R. (2008). Evaluation of ultrasonic snow depth sensors for US snow measurements. *Journal of Atmospheric & Oceanic Technology*, *25*(5), 667–684.

Sihvola, A. & Tiuri, M. (1986). Snow fork for field determination of the density and wetness profiles of a snow pack. *Geoscience and Remote Sensing, IEEE Transactions on*, *GE-24,*(5), 717–721.

Stacheder, M. (2005). TDR and low-frequency measurements for continuous monitoring of moisture and density in a snow pack. *International Agrophysics*, *19*, 75–78.

Stacheder, M., Koeniger, F., & Schuhmann, R. (2009). New dielectric sensors and sensing techniques for soil and snow moisture measurements. *Sensors*, *9*(4), 2951–2967.

Stähli, M., Stacheder, M., Gustafsson, D., Schlaeger, S., Schneebeli, M., & Brandelik, A. (2004). A new in situ sensor for large-scale snow-cover monitoring. *Annals of Glaciology*, *38*(1), 273–278.

Stein, J., & Kane, D. L. (1983). Monitoring the unfrozen water content of soil and snow using time domain reflectometry. *Water Resources Research*, *19*(6), 1573–1584.

Stein, J., Laberge, G., & Lévesque, D. (1997). Monitoring the dry density and the liquid water content of snow using time domain reflectometry (TDR). *Cold Regions Science and Technology*, *25*(2), 123–136.

Techel, F., & Pielmeier, C. (2011). Point observations of liquid water content in wet snow–investigating methodical, spatial and temporal aspects. *The Cryosphere*, *5*(2), 405–418.

Waldner, P., Huebner, C., Schneebeli, M., Brandelik, A., & Rau, F. (2001). *Continuous measurements of liquid water content and density in snow using TDR.* In Second International Symposium and Workshop on Time Domain Reflectometry for Innovative Geotechnical Applications, Evanston, IL (pp. 446–456).